Journal of Chromatography A, 1228 (2012) 2–19

Contents lists available at ScienceDirect

Journal of Chromatography A

journal homepage: www.elsevier.com/locate/chroma

The current revolution in column technology: How it began, where is it going?

Fabrice Gritti, Georges Guiochon*

Department of Chemistry, University of Tennessee, Knoxville, TN 37996-1600, USA

ARTICLE INFO

Article history:
Available online 23 July 2011

Keywords:
Column technology
Mass transfer mechanism
HETP
Monolithic column
Eddy diffusion
Trans-column effect
RPLC

ABSTRACT

This work revisits the exceptionally rapid evolution of the technology of chromatographic columns and the important progress in speed of analysis and resolution power that was achieved over the last ten years. Whereas columns packed with 10 and 5 μm fully porous particles dominated the field for nearly thirty years (1975–2000), it took barely six years to see the commercialization of monolithic silica rods (2000), their raise to fame and decay to oblivion, the development of finer fully porous particles with size down to 1.7 μm (2006), and of sub-3 μm superficially porous particles (2006). Analysis times and plate heights delivered by columns packed with these recent packing materials have then been improved by more than one order of magnitude in this short period of time. This progress has rendered practically obsolete the age-old design of LC instruments. For low molecular weight compounds, analysts can now achieve peak capacities of 40 peaks in about 15 s with a hold-up time of the order of 1.5 s, in gradient elution, by operating columns packed with sub-3 μm shell particles at elevated temperatures, provided that they use optimized high pressure liquid chromatographs. This is the ultimate limit allowed by modern instruments, which have an extra-column band broadening contribution of 7 μL^2 at 4.0 mL/min and data acquisition rate of 160 Hz. The best 2.1 mm × 50 mm narrow-bore columns packed with 1.7 μm silica core–shell particles provide peaks that have a variance of 2.1 μL^2 for $k = 1$. Finally, this work discusses possible ways to accelerate separations and, in the same time perform these separations at the same level of efficiency as they have today. It seems possible to pack columns with smaller particles, probably down to 1 μm and operate them with current vHPLC equipments for separations of biochemicals. Analyses of low molecular weight compounds will require new micro-HPLC systems able to operate 1 mm I.D. columns at pressures up to 5 kbar, which would eliminate the heat friction problems, and providing extra-column band broadening contributions smaller than 0.1 μL^2. Alternatively, a new generation of vHPLC systems with minimal extra-column contributions of less than 0.5 μL^2 could run 2.1 mm I.D. columns if these latter were to be packed with high heat conductivity materials such as core–shell particles made with an alumina or gold core.

1. Introduction

Column technology has evolved as fast during the last decade as in the decade of the discovery of HPLC, between early 1960s and 1970s. In contrast, between 1975 and 2000, the conventional columns were 4.6 mm I.D. stainless steel tubes packed with spherical particles having between 10 and 5 μm in diameter. Their length slowly decreased from 300 to 150 mm. The minimum plate height of the commercial columns packed with 5 μm particles was around 12 μm ($h \simeq 2.3$) [1]. Their specific permeability was typically about 2×10^{-14} m^2, the hold-up volume of 250 mm × 4.6 mm columns was close to 2.5 cm^3, and their optimum column impedance ($H^2_{min}\epsilon_t/k_0$, with $\epsilon_t = 0.60$) nearly 4500. Progressively, home-packed columns were replaced with commercial columns, publications on packing technology progressively vanished, column manufacturers kept their technical advances confidential, and it seemed that column technology froze. Fine porous particles (1.5–2 μm diameter) were prepared and used by several research groups [2,3] but they never entered into the commercial market.

Then, in 1999, Merck commercialized the first 100 mm × 4.6 mm monolithic silica columns (Chromolith) [4]. In the late 1990s, Nakanishi and Tanaka had developed a method for the preparation of such columns based on the hydrolysis of tetramethoxysilane in an acidic solution, in the presence of a suitable porogen (e.g., polyacrylic acid, polyethylene oxide), followed by the maceration of the gel in a basic solution leading to the formation of suitable mesopores [5]. These new columns were made of a single block of silica, with a bimodal pore size distribution, encapsulated in a PEEK tube [6]. These columns had over conventional packed columns the major advantage that the average pore size of each mode could

* Corresponding author. Tel.: +1 865 974 0733; fax: +1 865 974 2667.
E-mail addresses: guiochon@utk.edu, guiochon@ion.chem.utk.edu (G. Guiochon).

0021-9673/$ – see front matter © 2011 Elsevier B.V. All rights reserved.
doi:10.1016/j.chroma.2011.07.014

be adjusted independently. The size of the large pores (throughpores or macropores) was set around 2 μm and the corresponding porosity around 0.7, providing a high column permeability and allowing the flow of the mobile phase to take place with a minimal pressure drop along the column. The size of the small pores (mesopores) was fixed around 130 Å, generating a sufficiently large specific surface area (300 m^2/g) for retention purposes [7]. The permeability of these monolithic rods is around 8×10^{-14} m^2 [8]. The minimum plate height correctly measured by the numerical integration method is around 15 μm [8,9], but values measured using the erroneous half-height peak width method have provided more generous estimates, around 8 μm [8,10–12]. Accordingly, the true minimum column impedance is close to 2400, twice smaller than that of columns packed with 5 μm particles. In the early 2000s, these columns appeared to be a very promising alternative to packed columns. They opened the way to faster HPLC analyses because mass transfer resistances were much lower than in packed columns (but, unfortunately, they have a large eddy diffusion contribution to band broadening). Their use could have permitted large increases in analytical throughputs, with analysis times at constant resolution nearly four times lower than that of columns packed with 5 μm particles. These columns generated much enthusiasm among scientists and a limited interest among practitioners. Eventually, interest faded and monolithic columns seem to be on their way to oblivion. They may be revived if considerable progress is made in their preparation, making them radially homogeneous. Long, narrow (d_c < 0.5 mm) monolithic columns might also be most useful if operated at low linear velocities to provide ultrahigh efficiency separations.

However, under the combined pressures of the need of the pharmaceutical industry requiring large increases in analytical throughputs and of the threat of the competition brought by these monolithic columns, the established manufacturers of packing materials began to produce and commercialize columns packed with fully porous particles of decreasing sizes, 5, then 3.5, 2.5, and eventually 1.7 and 1.5 μm. Columns became shorter, down to between 50 and 150 mm, yet they are as or more efficient than former ones. To cope with the resulting decrease of the decreasing permeability of columns packed with finer particles, instrument manufacturers had to develop new pumps able to operate at pressures as high as 1000 bar or even higher. Eventually, very high-pressure liquid chromatography (vHPLC) was born in 2004 while narrow-bore (2.1 mm I.D.) short (50 mm long) columns became popular. The minimum HETP of columns packed with sub-2 μm particles dropped to ca. 3.5 μm [13–15], with permeabilities close to 2.5×10^{-15} m^2 [14,15] and minimum column impedance (total porosity ϵ_t = 0.60) around 3000.

In practice, a 4.6 mm I.D. 15 cm long column made of a monolithic silica rod (Onyx-C_{18} column at 200 bar [9]) and a 4.6 mm I.D. 7 cm long column packed with 1.7 μm fully porous particles (BEH-C_{18} column at 1000 bar [9,15]) can be operated to give the same hold-up time of 10 s with a mobile phase of viscosity 0.72 cP (acetonitrile/water, 65/35, v/v, at 295 K) . Their respective plate numbers would be 2200 and 10 500. Thus, a more than twice larger resolution can be achieved in vHPLC than with highly permeable monolithic columns in ultra-fast chromatography. This explains why the earlier hopes invested in the use of monolithic columns in liquid chromatography suddenly vanished a few years ago. This result is essentially explained by the relatively poor efficiency of monolithic columns, due to the radial heterogeneity of the silica rods combined with a rather poorly designed sample distributor [16–19]. A long awaited second generation is still hoped for.

The second leap forward in column technology came a few years later with the introduction by Advanced Material Technologies (Wilmington, DE, USA) of particles developed after the old concept of pellicular particles unsuccessfully implemented of the 1970s, when the particle size was 50 μm and the shells made of aggregates of nanoparticles were only a few μm thick [20–22]. In contrast, the 2.7 μm Halo particles [23] provide a satisfactory sample loading capacity (the volume of the porous shell represents about 75% of the particle volume), their permeability is ca. 6.0×10^{-15} m^2 and their minimum HETP as low as 3.4 μm [24–27]. These columns provide an impedance around 1000. A few other core–shell particle brands have since been commercialized, Kinetex in 2009, Poroshell 120 in 2010 and several research groups have made similar products [28,29]. The most significant advantages of columns packed with sub-3 μm shell particles over those packed with sub-2 μm fully porous particles are their relatively larger permeabilities and the marked decrease of the heat friction effects [30,31]. Remarkably, a hold-up time as small as 10 s can be obtained with an inlet pressure of only 400 bar and an 8 cm long column, giving a plate count of 16 000 under the same conditions as above [27]. Therefore, provided that instruments that have sufficiently low extra-column volume contributions to band broadening are available [32], columns packed with shell particles can allow very fast separations, with resolution comparable to or even slightly larger than those packed with very fine fully porous particles.

The purpose of this work is to investigate the different approaches which may allow analysts to achieve very fast, yet highly efficient separations by unidimensional HPLC. We discuss in details the contributions of possible modifications in the physico-chemical properties of the eluents (due to temperature and pressure adjustments) and those that could arise from further developments of new stationary phases. This work is based on measurements of accurate column plate heights by numerical integration of the experimental peak profiles [33] recorded for standard commercially available columns with instruments currently available. The columns and packing materials considered for the typical examples of possible results that we provide are the 5 μm fully porous Luna-C_{18}(2) 150 mm × 4.6 mm, the Onyx-C_{18} 100 mm × 4.6 mm monolithic column, the 1.7 μm fully porous BEH-C_{18} 50 mm ×2.1 mm, and the superficially porous 2.7 μm Halo-ES-peptide 150 mm × 4.6 mm columns. In conclusion, we summarize the gains in speed and efficiency that were achieved during the last ten years, provide estimates of the current ultimate speed that could now be achieved with the latest HPLC columns and instruments now available, and discus the possible and probable improvements that the miniaturization of HPLC could afford during the next decade.

2. Theory

In the first part of the theory section, we briefly summarize the classical chromatographic equations that relate the speed of a separation to the resolution power of the column, as described by Poppe [34]. Then we discuss what means are available to perform faster and more efficient separations.

2.1. Speed–efficiency relationship: the Poppe plot

The primary objective of separation analysts is to identify a maximum number of analytes in the minimum amount of time and to derive an accurate quantitative estimate of their concentrations. This sets a definition of the resolving power of a chromatographic method as the ratio of the hold-up time to the nominal column efficiency. Although generally used, the term of column efficiency is often defined loosely and might be misleading because the column efficiency is measured for a given compound and its exact value might change significantly from one compound to the next.

Poppe developed a straightforward method of comparison between different chromatographic approaches to the achievement of a given separation that consists in plotting t_0/N as a function of the column efficiency N. From a general viewpoint, consider u_S the superficial linear velocity and $H(u_S)$ the associated plate height correlation. The hold-up time and the column efficiency are given by

$$t_0 = \frac{\epsilon_t L}{u_S} \tag{1}$$

where ϵ_t is the total porosity of the column, and by definition:

$$N = \frac{L}{H(u_S)} \tag{2}$$

HPLC is always conducted under laminar conditions, so the pressure and the mobile phase velocity are related through the Darcy equation:

$$\frac{\Delta P}{L} = \frac{\eta}{k_0} u_S \tag{3}$$

where ΔP is the pressure drop between the column inlet and outlet, η is the viscosity of the mobile phase, and k_0 is the specific permeability of the chromatographic bed, which is mostly a function of the external bed porosity and of the average particle size.

Using Eqs. (2) and (3) to eliminate the variable L and assuming that the plate height, $H(u_S)$, is independent of the column length, the column efficiency is rewritten:

$$N = \frac{k_0}{\eta} \frac{1}{u_S H(u_S)} \Delta P \tag{4}$$

By combining Eqs. (1) and (2) to eliminate the column length, L, the resolving power can be written as:

$$\frac{t_0}{N} = \frac{\epsilon_t H(u_S)}{u_S} \tag{5}$$

The Poppe plots are simply derived from the van Deemter curves of the columns compared, $H = f(u_S)$. Once the experimental data are fitted to the empirical van Deemter model ($H = (B/u_S) + A + Cu_S$), the complete Poppe plot are drawn for any arbitrary value of the pressure drop, the choice of which depends on the HPLC system used (with maximum inlet pressures of 400 or 1000 bar depending on whether conventional HPLC or vHPLC are considered) or on the column pressure tolerance (e.g., 200 bar for monolithic columns), assuming a given column permeability k_0, which accounts for the nature of the stationary phase (large or small particles, monolithic supports) and a fixed mobile phase viscosity η, which depends on the temperature, the eluent composition and state (liquid or supercritical).

2.2. Conditions for the validity of the Poppe plots and their conclusions

One important assumption made in drawing the Poppe plots is that the product $u_S L$ remains a constant over the whole plot. The conclusions derived from a Pope plot are valid only if (1) the efficiency remains the same for all the components of the mixture considered; (2) the viscosity and the density of the mobile phase do not vary significantly with the pressure; and (3) provided that columns of different lengths can be packed with the same HETP, an assumption that is not supported by experimental results [35] and should be considered as approximate.

Therefore, any point in a Poppe plot (t_0/N, N) is a mere extrapolation of the actual experimental data (u_S and H) acquired using a single column and a series of increasing pressure drops (10–400 bar). This extrapolation is based on the assumptions that (1) the HETP is independent of the column length; and (2) the density and the viscosity of the eluent are independent of the pressure. While these assumptions are somehow valid for low or moderate values of the column inlet pressure (<300 bar), they are obviously questionable for the much larger pressures encountered in vHPLC, because (1) liquids are compressible [36–39]; (2) their viscosity increases with increasing pressure [39,40]; and (3) at high velocities, the apparent column HETP is affected by the frictional heat effects [41–43] and is no longer independent of the column length [14,15]. In conclusion, the position of all the points in a Poppe plot is subject to a degree of error that varies with the experimental conditions assumed and is difficult to estimate. Obviously, all these restrictions apply as well to any of the kinetic plots which were recently derived from the Poppe plot concept and do not bring anything new to it. Yet, the advantage of the Poppe plots is that they provide useful qualitative information when comparing the performance of two different chromatographic systems that differ in the physico-chemical properties of either the mobile phase (temperature, viscosity) or the packing material (permeability, particle diameter).

Finally, note that, in fast elution chromatography, we are interested in short columns operated at high linear velocities, e.g. mostly in the bottom left region of these plots.

2.3. From a theoretical viewpoint, which approach might be effective for doing fast chromatography?

The ultimate goal in fast chromatography is to decrease the hold-up time of the column (Eq. (1)) while keeping its efficiency (Eq. (2)) as high as possible. The solutions to this problem are straightforward: we can either decrease the column length and the column plate height in the same time or we can increase the linear velocity of the mobile phase at constant efficiency. Overall, this leads to five different experimental approaches:

1. The linear velocity can be increased by decreasing the viscosity of the eluent. Therefore, operating the column at an elevated temperature and/or with a supercritical fluid eluent are suitable options. In the same time, the diffusion coefficients being inversely proportional to the viscosity increase, making mass transfer faster. So, these two approaches are attractive.
2. More simply, the linear velocity can be increased by operating the column under a higher inlet pressure. The success of the outcome of this option depends on the slope of the C-branch of the van Deemter curve of the column at high velocities.
3. The permeability of the column could be increased, allowing the use of a higher flow rate with the same inlet pressure. This is what made monolithic columns so attractive. The success of this option depends on the level of column efficiency that can be achieved with these highly permeable columns.
4. The column length can be reduced if the plate height is decreased, e.g. by decreasing the mean particle size. This is the rationale behind the past development of finer particles, from 10 to sub-2 μm particles. However, in the same time, the permeability of the column decreases in proportion to the reverse of the particle diameter squared. Therefore, this third option is intimately linked with the second option, e.g. the application of very high pressures.
5. Finally, a combination between an increase of the column permeability (option 3) and of its efficiency (option 4) is also possible, as illustrated by the development of the sub-3 μm shell particles, which now compete with the sub-2 μm fully porous particles. Fast separations are then possible without the constraints of very high pressures.

These different options will be explored in detail in Section 4 of this work.

2.4. Determination of the true experimental HETP $H(u_S)$

Significant errors can be made if inappropriate, inaccurate methods are chosen to measure the column HETP. Actual peak profiles are rarely Gaussian and they cannot be accurately fitted to any of the mathematical peak functions that have been suggested so far in the literature [33].

We calculate the plate height as it is defined in the general rate model, from the first and the second central moments of the elution profiles. To correct for the band broadening contribution of the extra-column volumes of the instrument, elution bands are recorded at a series of flow velocities first with the column fitted to the instrument and then, at the same velocities, with the column being replaced by a zero-volume connector. The moments of the peak profiles eluted through the extra-column volume and through the overall (system + column) are measured by numerical integration of the full concentration profiles. To reduce the noise and improve the precision of the measurements, a fraction of the data points at the left and at the right of the peak are excluded from the numerical calculations, as explained elsewhere [33]. The left and the right cuts are determined from the moments when the average slope of the signal decay measured over $Z/200$ consecutive points is larger than or equal to zero, with Z being the number of points recorded for the peak profile. The number 200 was arbitrarily chosen; it is the minimum number of data points required to describe a baseline length equal to six times the variance of the peak profiles or about 30 data points per standard deviation. In a second step, the peak profile is corrected for the linear baseline drift determined from the slope of the line joining the left and the right cut points. The first and the second central moments of the concentration profiles were calculated in an Excel spread-sheet using the data points acquired. They are given by:

$$\mu_1 = \frac{\sum_{i=1}^{i=Z-1} (C_i + C_{i+1})(t_i + t_{i+1})}{2\sum_{i=1}^{i=Z-1} C_i + C_{i+1}} \quad (6)$$

$$\mu'_2 = \frac{\sum_{i=1}^{i=Z-1} (C_i + C_{i+1})((t_i + t_{i+1}/2) - \mu_1)^2}{\sum_{i=1}^{i=Z-1} C_i + C_{i+1}} \quad (7)$$

The corrected HETP, H, is then given by the equation [44]:

$$H = L\frac{\mu'_2 - \mu'_{2,ex}}{(\mu_1 - \mu_{1,ex})^2} \quad (8)$$

where L is the column length and $\mu_{1,ex}$ and $\mu'_{2,ex}$ are the first and the second central moments of the corresponding extra-column band profiles. As demonstrated previously, this method is correct and should always be preferred to the incorrect, approximate, and inaccurate method consisting in measuring the peak widths at mid-height [33], even if this latter method is often more precise than the former. A gain in precision might not be obtained at the cost of a loss of accuracy. The precision of the H data is given by

$$\left|\frac{\Delta H}{H}\right| = \left|\frac{\Delta\mu'_2}{\mu'_2}\right|\left(\frac{\mu'_2 + \mu'_{2,ex}}{\mu'_2 - \mu'_{2,ex}}\right) + 2\left|\frac{\Delta\mu_1}{\mu_1}\right|\left(\frac{\mu_1 + \mu_{1,ex}}{\mu_1 - \mu_{1,ex}}\right) \quad (9)$$

The reproducibility achieved is typically better than ±5% for retained compounds and around ±10% with non-retained compounds.

3. Experimental

3.1. Chemicals

The mobile phases were all mixtures of acetonitrile or methanol and water. Tetrahydrofuran was also used as the eluent for porosity measurements by inverse size-exclusion chromatography (ISEC). All these pure eluents were HPLC grade from Fisher Scientific (Fair Lawn, NJ, USA). The mobile phases were filtered before use on a surfactant-free cellulose acetate filter membrane, 0.2 μm pore size (Suwannee, GA, USA). Eleven polystyrene standards (MW = 590, 1100, 3680, 6400, 13 200, 31 600, 90 000, 171 000, 560 900, 900 000, and 1 877 000) were used to acquire the ISEC data. They were purchased from Phenomenex (Torrance, CA, USA). The small compounds used for the measurement of the column HETPs in this work were phenol (Luna-C_{18}(2) column), naphthalene (Onyx-C_{18} and Halo-ES-Peptide-C_{18}), and naphtho[2,3-a]pyrene (BEH-C_{18}) with a minimum purity of 99% (Fair Lawn, NJ, USA).

3.2. Apparatus

All the necessary and detailed information regarding the HPLC instruments (extra-column parts including the injection volume, the connecting capillaries, and the detector cell) used can be found in Refs. [1,9,15,45,46] for the measurement of the data regarding the Luna-C_{18}(2), the Sunfire-C_{18}, the Onyx-C_{18}, the BEH-C_{18}, and the Halo-ES-Peptide-C_{18} column, respectively.

3.3. Columns

The 5 μm fully porous Luna-C_{18}(2) (150 mm × 4.6 mm) and Onyx-C_{18} (100 mm × 4.6 mm) columns were purchased from Phenomenex (Torrance, CA, USA). The 5 μm fully porous Sunfire-C_{18} (150 mm × 4.6 mm) and 1.7 μm fully porous BEH-C_{18} (50 mm × 2.1 mm) columns were given by Waters (Mildford, MA, USA). Finally, the superficially porous 2.7 μm Halo-ES-peptide 150 mm × 4.6 mm packed columns was kindly given by Advanced Material Technologies (Wilmington, DE, USA) for the sake of the evaluation of its kinetic performance.

3.4. HETP plots

The HETP data were all corrected for the extra-column contributions of the HPLC system. The eluents were a mixture of methanol and water (10/90, v/v, sample phenol, column Luna-C_{18}(2)), a mixture of acetonitrile and water (55/45, v/v, sample naphthalene, column Onyx-C_{18}), pure acetonitrile (sample naphtho[2,3-a]pyrene, column BEH-C_{18}), a mixture of acetonitrile and water (20/80, v/v, sample naphthalene, column 2.7 μm Halo-ES-peptide), and a mixture of acetonitrile and water (15/85, v/v, sample phenol, column Sunfire-C_{18}). The temperature was ambient, except for the Sunfire column for which the influence of the temperature over the range from 21 °C to 77 °C on the HETP was investigated [1]. For more details regarding the sequence of the flow rates applied, the reader is referred to the above-cited papers [1,9,15,45,46]. The first and second central moments of all peaks were accurately measured using the numerical integration method.

3.5. ISEC experiments

The external porosities of the four tested columns were derived from the results of ISEC measurements. Neat THF was used as the eluent. Twelve polystyrene standards with molecular weights between 100 and 2 millions Dalton were used as the probe compounds. This covers a wide range of molecular sizes (hydrodynamic diameter) between 4 and 950 Å. The average mesopore

size expected before C_{18} derivatization is close to 90 Å. The external porosity was determined from the extrapolated elution volumes of the exclusion branches, to a molecular radius of zero, divided by the column tube volume. The total porosity was measured according to pycnometric measurements [47,48]. All the results are listed in Table 1.

4. Results and discussion

In the first part of this section, we report and discuss the possibilities and the limitations of the options 1–5 listed in the theory section for the achievement of faster and still high resolution separations by HPLC. In the second part, we estimate the highest speed and the peak capacity that can be experimentally obtained today in unidimensional ultra-fast gradient elution, given the currently available columns and HPLC instruments. Finally, we estimate the possibility of a further decrease of the column length and the particle size with respect to the analysis of small and large molecules.

4.1. Practical options to increase speed and resolution in 1D HPLC

The use of elevated temperatures, ultra-high pressures, monolithic columns, sub-2 μm particles, and sub-3μm superficially porous particles are described and discussed. Their impact on the increase of the speed of analysis and on the resolution power are discussed and their limitations are exposed.

4.1.1. Elevated temperature

Increasing the temperature at which HPLC separations are performed allows analysts to use longer columns at a fixed pressure drop because the eluent viscosity, η decreases rapidly with increasing temperature. Fig. 1 shows the impact of an increase in the temperature on the viscosity of mixtures of acetonitrile and water.

A rather mild increase of the temperature from ambient (ca. 20 °C) to about 50 ° C causes a significant decrease of the viscosity of aqueous solutions of acetonitrile, by nearly a factor two. The same conclusion applies to mixtures of methanol and water [49,50]. Accordingly, it becomes possible either to use a twice longer column at the same linear velocity and to achieve an approximately twice larger efficiency or to operate the same column at an approximately twice faster flow rate, which would provide about twice faster analyses, with roughly the same efficiency using the same column, providing that the first separation was made with a mobile phase velocity only moderately higher than the optimum velocity for maximum efficiency.

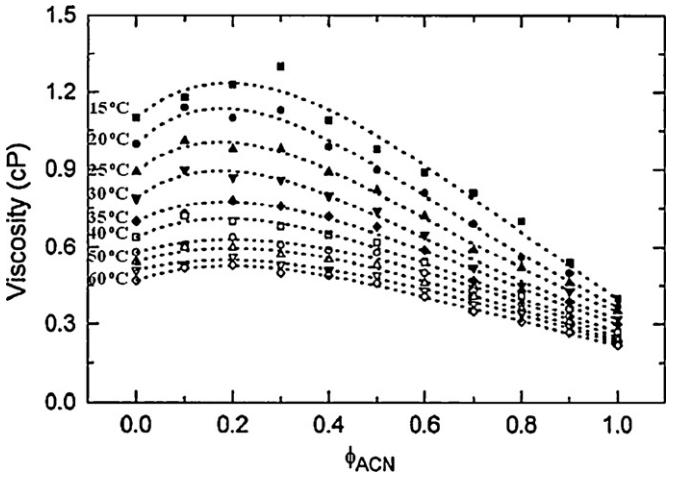

Fig. 1. Effect of the temperature on the viscosity of mixtures of acetonitrile and water. Reproduced from Ref. [49].

Table 1
Physico-chemical properties of the chromatographic columns tested in our lab.

	Sunfire	Luna	Onyx	BEH	Halo
Neat silica					
Mean particle size [μm]	5	4.9	2.8 (domain size) Skeleton size 0.8 μm Throupore size 2.0 μm	1.7	2.7
$\rho = R_i/R_e$	1.00	1.00	1.00	1.00	0.63
Pore diameter [Å]	90	100	130	130	160
Surface area [m^2/g]	349	427	300	185	80
Particle size distribution ($d_{90-10\%}$)	1.55	1.9	–	1.5	1.1
Packed columns analysis					
Batch/Serial number	108/0108143281	5291-72/405594-19	8191-44/080620-54	0167290202 0A01	BH092206/USKF001250
Dimension (mm × mm)	4.6 × 150	4.6 × 150	4.6 × 100	2.1 × 50	4.6 × 150
External porosity [b]	0.37	0.36	0.71	0.37	0.40
Total porosity [a]	0.62	0.64	0.82	0.66	0.56
Specific permeability[c], k_0 [cm^2] (eluent used)	6.0×10^{-10} (CH_3CN/H_2O, 15/85)	2.4×10^{-10} (H_2O)	6.2×10^{-10} (CH_3CN/H_2O, 55/45)	2.6×10^{-11} (CH_3CN)	6.1×10^{-11} (CH_3CN/H_2O, 20/80)

[a] Measured by pycnometry (THF-CH_2Cl_2).
[b] Measured by inverse size exclusion chromatography (polystyrene standards).
[c] Measured from the total back pressure data corrected for extra-column contributions at room temperature.

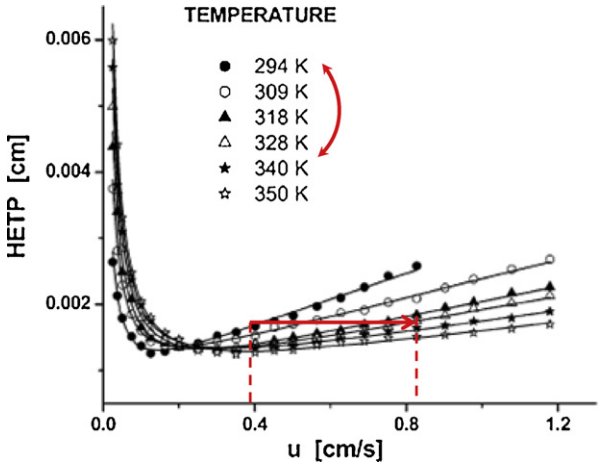

Fig. 2. Effect of the temperature on the HETP of a 5 μm Sunfire-C_{18} column for phenol eluted with a mixture of acetonitrile and water (15/85, v/v). The eluent viscosity decreases from 1.09 to 0.37 cP when the temperature increases from the ambient temperature to 77 °C.

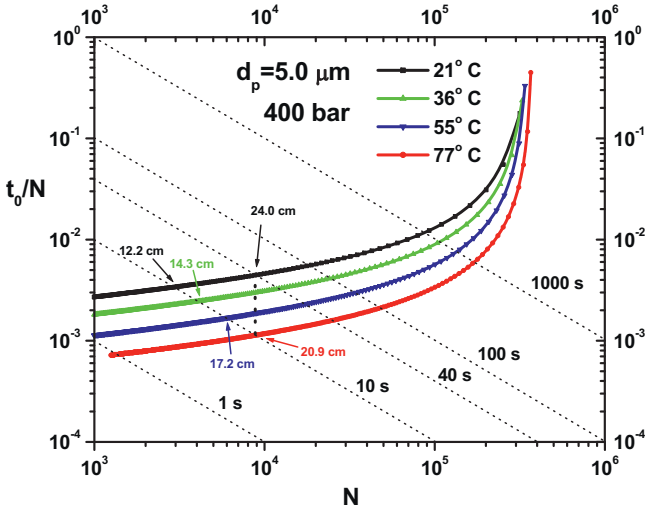

Fig. 3. Effect of the temperature on the Poppe plot of phenol for columns packed with 5 μm Sunfire-C_{18} particles, eluted with a mixture of acetonitrile and water (15/85, v/v). The pressure constraint was set at 400 bar. Note the three-fold increase of the efficiency at constant hold-up time and the four-fold decrease of the analysis time at constant column efficiency when the temperature increases from the ambient temperature to 77 °C.

Fig. 2 illustrates how it is possible to double the linear velocity of the mobile phase when the temperature is increased from 21 to 55 ° C at constant column HETP [1]. The data for this figure were measured with phenol eluted with a mixture of acetonitrile and water (15/85, v/v) on the Sunfire-C_{18} packed column (Section 3.3).

In order to built and compare the complete Poppe plots at various temperatures, it is necessary to measure the actual influences of the temperature on the viscosity and on the column HETP. Thus, the impact of the temperature on the longitudinal diffusion coefficient B (e.g., on the diffusion coefficient, D_m and the effective sample diffusivity through the porous particles, ΩD_m), on the eddy diffusion term, A, and on the solid–liquid mass transfer resistance coefficient, C, should be known.

The variation of the mobile phase viscosity with the temperature is well approximated by the following equation [51]:

$$\eta(T) = 10^{(A_\eta + (B_\eta/T))} \tag{10}$$

For instance, $A_\eta = -5.89$ and $B_\eta = 861$ K for a mixture of acetonitrile and water (15/85, v/v) in the temperature range between 15 ° C and 60 ° C [49].

The diffusion coefficient D_m is given by the following kind of equation:

$$D_m(T) = D_m(T_{ref})\frac{\eta(T_{ref})}{\eta(T)}\frac{T}{T_{ref}} \tag{11}$$

where T_{ref} is the reference temperature at which the diffusion coefficient of the sample is known. Eq. (11) was assumed to be true in liquids, in the temperature range between the ambient temperature and 350 K. This correlation was recommended by Reid, Prausnitz, and Poling [51]. Assuming a simple parallel diffusion model in the packed bed (a model in which the contributions or rather the mass fluxes of diffusion in the interstitial volume and of diffusion in the porous particles are added), the variation of the parameter Ω with the temperature can be empirically derived from the data given in Ref. [1] for a column packed with the Sunfire-C_{18} particles immersed in a 15/85, v/v acetonitrile/water mixture, giving:

$$\Omega(T) = -6.97 + 0.0631T - 1.10 \times 10^{-4}T^2 \tag{12}$$

where T is the absolute temperature.

Actually, a satisfactory approximation for the A term in the van Deemter equation is provided by the following expression that lumps the contributions of the trans-channel, the short-range interchannel, and the trans-column velocity biases [52]. According to the data reported in Ref. [1], the dependence of the A coefficient on the temperature can be written as

$$A(T) \simeq \frac{1}{(1/2\lambda d_p) + (D_m(T)/\omega d_p^2 u_S)} \tag{13}$$

where the best values for λ and ω are 0.8 and 1.0, respectively.

Finally, the equation providing the overall solid–liquid mass transfer resistance term gathers the contributions of the external mass transfer resistance (H_{Film}) and that of the trans-particle mass transfer resistance ($H_{stat.}$). It is given by [1]:

$$\frac{H_{Film} + H_{stat.}}{d_p} = \frac{\epsilon_e}{1-\epsilon_e}\left(\frac{k_1}{1+k_1}\right)^2\left(\frac{F_{Film}}{3.27}\nu_S^{2/3} + \frac{1}{\Omega}\nu_S\right) \tag{14}$$

where F_{Film} was empirically measured as 3.1 [1].

Fig. 3 shows the Poppe plots derived for phenol from the experimental HETP data obtained for the Sunfire-C_{18} column (Section 3.3) eluted with a mixture of acetonitrile and water (15/85, v/v) at different temperatures, 21, 36, 55, and 77 °C. Obviously, all the points in Poppe plots are virtual points (see Section 2.2). The only measurements of HETP data actually made were obtained with one single column of length L = 15 cm, at a series of mobile phase velocities corresponding to increasing pressure drops from 10 to 400 bar. In contrast, a Poppe plot is supposed to be built for a constant pressure drop (in Fig. 3, the constant pressure was set at 400 bar) and for any possible column lengths. The shorter the column length, the faster the analysis (the higher the linear velocity) and the smaller the column efficiency. Conversely, the smaller the linear velocity, the longer the column length and the larger its efficiency.

When the column length tends toward infinity and the linear velocity tends toward zero, all the curves in a Poppe plot converge toward a limit vertical asymptote and a number of theoretical plates that is function of the accepted pressure limit, the column permeability and the eluent viscosity. For slow separations, the column efficiency is controlled by the longitudinal diffusion coefficient, B, and, according to Eq. (4), this limiting efficiency is

$$N = \frac{k_0}{B\eta}\Delta P \tag{15}$$

Because the B coefficient is approximately proportional to D_m, itself inversely proportional to the eluent viscosity, η, the product $B\eta$

depends weakly on the temperature. In the case of Fig. 3, the limit efficiency is close to 400 000 plates. Typically, we expect that the average values of B is close to $2D_m = 3.7 \times 10^{-5}$ cm^2/s [53,1]. The other characteristics of the system used to measure the data shown in Fig. 2 are $\eta = 6 \times 10^{-3}$ g cm^{-1} s^{-1}, $k_0 \simeq 2.5 \times 10^{-10}$ cm^2. Therefore, for a 400 bar pressure drop, the highest possible efficiency predicted would be close to 450 000, in good qualitative agreement with Fig. 3.

In fast chromatography, the relevant part of the Poppe plot is its bottom left corner, which corresponds to high separation speeds. For instance, if the analyst sets a hold-up time around 10 s, this speed could be achieved with either a 12.2 cm long column operated at 21 ° C or with a much longer 20.9 cm column operated of 77 °C, with the same eluent, under the same pressure, which provides a three-fold gain in efficiency (from 2890 to 8800 plates) and a peak resolution increased by a factor 1.75. Alternately, if the analyst is primarily interested in resolution with a plate number around 9000, this performance could be achieved with either a 24 cm long column operated at 21 ° C or with a 20.9 cm column at 77 °C. The advantage of operating at the higher temperature is the four times shorter analysis time, since the mobile phase viscosity decreases from 1.09 to 0.37 cP and the hold-up time decreases from 40 to 10 s.

The main limitations to the use of high temperatures in liquid chromatography are due to the limited chemical stability of the stationary phase and the sample components. This problem is particularly critical with silica-bonded phases operated under extreme pH conditions (pH < 1 or pH > 9 at temperatures larger than 50 °C). This problem could be solved by replacing the traditional columns packed with silica-based particles by other more chemically and thermally stable metal oxides such as zirconium or aluminum [54–58] or by polymeric based particles. High temperatures can also affect the detector response in different ways.

In conclusion, elevating the eluent temperature is certainly the cheapest alternative to speed up analytical separations and generate more plate counts by using longer columns.

4.1.2. Supercritical fluid chromatography (SFC)

An alternative to the use of high temperatures in order to decrease the mobile phase viscosity and increase the speed of separations consists in using a very dense gas or a supercritical fluid as the mobile phase. Neat carbon dioxide or its mixtures with organic modifiers make attractive mobile phases, with a viscosity between 0.02 (low density, 0.2 g/cm^3) and 0.12 cP (high density, 1.0 g/cm^3) for pure CO_2. This fluid is at least three times less viscous than the least viscous HPLC solvent, acetonitrile (viscosity 0.37 cP at room temperature), despite its larger density (1.0 *versus* 0.8 g/cm^3). Accordingly, the advantage of using CO_2 as a mobile phase is clear in fast chromatography.

In so far as it makes sense to draw a Poppe plot in SFC, graphs similar to the one shown in Fig. 3 should be expected. For example, the plots in Fig. 4 illustrate the theoretical advantage of using neat CO_2 instead of a mixture of acetonitrile and water (15/85, v/v) and at the same temperature of 50 °C, and for a pressure drop of 400 bar at which the viscosity of pure CO_2 is 0.098 cP. The plot predicts a twice larger peak resolution at a fixed hold-up time of 10 s. The use of SFC would allow the use of much longer columns than that of HPLC (40 cm *versus* 15 cm). For a given level of efficiency ($N \simeq 30\,000$), SFC would reduce the analysis time by a factor 6. Although the application of the Poppe plot to SFC is arguable since diffusion coefficients of analytes depend much on the local pressure, which may vary considerably along the column despite the low viscosity, this result is consistent with the general observations of analysts that separations carried out by SFC are nearly five times faster than similar separations made on the same column by HPLC [59].

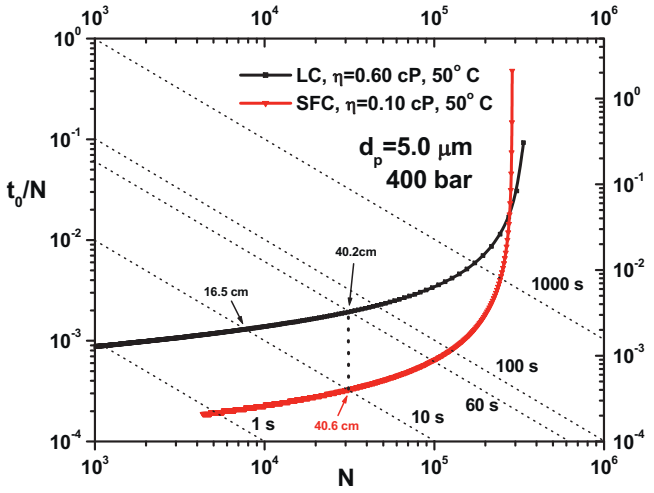

Fig. 4. Expected effect of the supercritical mobile phase CO_2 on the Poppe plot of phenol using a 5 μm Sunfire-C_{18} stationary phase. The pressure drop constraint was set at 400 bar. Note the four-fold increase of the efficiency at constant hold-up time and the six-fold decrease of the analysis time at constant column efficiency when the liquid eluent (CH_3CN/H_2O, 15/85, v/v) is replaced by neat CO_2 at the same temperature of 50 °C.

Because the viscosity of carbon dioxide is particularly low around the critical point, analysts might be tempted to operate columns in this region. However, such separations are often reported to produce low efficiency chromatograms [60]. The reason is that under certain such conditions, the column cannot be kept isothermal [59,60]. Due to the pressure drop along the column, the mobile phase expands and this expansion is endothermic. In the region around the critical point, the isobaric thermal expansion coefficient, α_P, of CO_2 ($\simeq$0.04 K^{-1} at 50 ° C and 100 bar) is about fifty times larger than that of pure liquid acetonitrile ($\simeq$0.0008 K^{-1}) [60]. Far away from the critical point, it is closer to the conventional values of solvents. As a result, the decompression of the mobile phase CO_2 is accompanied by an important decrease of its own temperature [42,61,60]. For instance, assume a pressure drop of 25 bar along a column packed with 5 μm particles and kept close to 305 K [62,63], then the temperature of the eluent decreases by about 13 K. If the column is left in direct contact with air, heat diffuses across the column diameter to the oven outside and a radial temperature gradient forms [41]. The thermal conductivity of CO_2 at 50 ° C and 100 bar is close to 0.06 W/m/K. Assume a flow rate of 1.265 mL/min and a column length of 15 cm [62], the amplitude of the radial temperature gradient could be as high as 5.5 K or higher across a column radius of 1 mm [64]. However, the thermal diffusivity of CO_2, which is in energy transfer the momentum equivalent of molecular diffusivity to mass transfer becomes very low near the critical point [60]. The chromatographic consequences in terms of column efficiency are dramatic if the column cannot be kept under adiabatic conditions [60,64].

Fig. 5 (top graph) illustrates the increasing deterioration of the peak shapes as the retention of compounds increases. It might be possible to cope with this cooling effect as it was possible to reduce the effects of the release of heat friction by encapsulating the column with fiberglass and foam pipe material [15,61]. Then, the apparent experimental efficiency for n-octadecane measured at a flow rate of 1.265 mL/min with a 150 mm × 2.0 mm column (u_S = 0.67 cm/s) is 10 500. In theory, assuming $D_m = 1.5 \times 10^{-4}$ cm^2/s for the bulk diffusion coefficient of n-octadecane in pure CO_2 at 50 ° C and at the average column pressure of 106 bar (η = 0.032 cP), the expected efficiency should have been around 12 200. The difference might be ascribed to an error in the estimate of D_m. In conclusion, 86% of the maximum theoretical efficiency could be obtained when

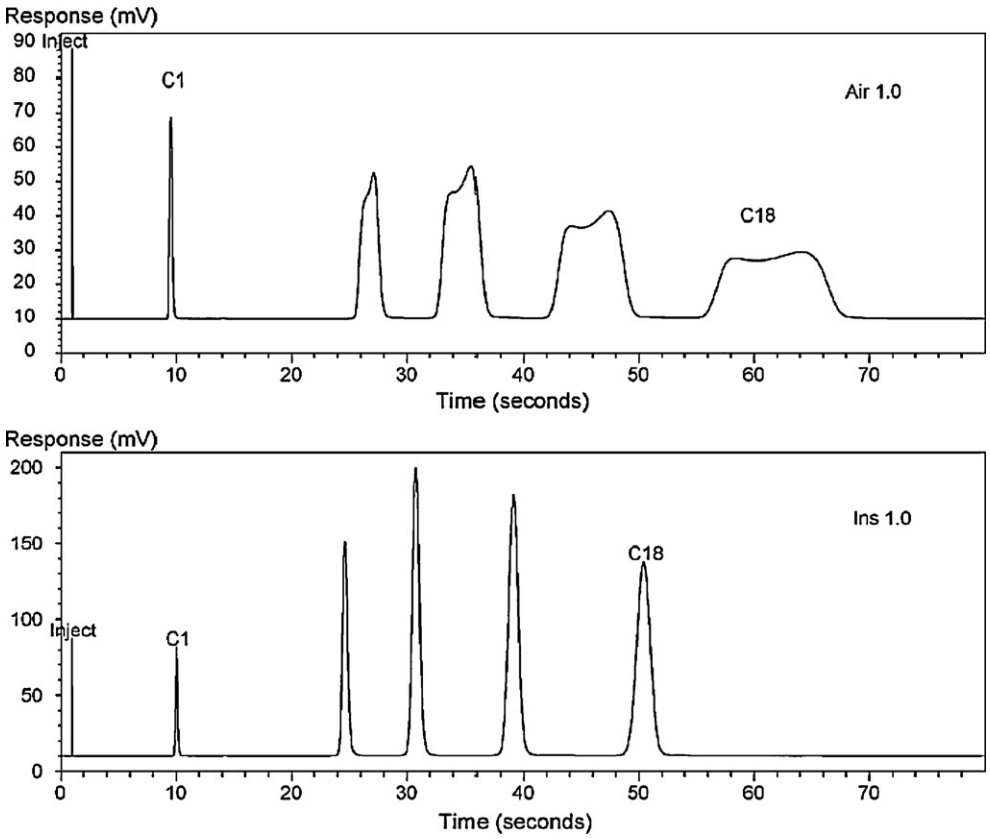

Fig. 5. Peak distortion observed in SFC. Mobile phase: neat CO_2. 2.0 mm × 150 mm column packed with 5 μm Spherisorb-C_8. Inlet pressure: 118.4 bar. Outlet pressure: 93.5 bar. T = 50 °C. Flow rate: 1.265 mL/min. Top graph: the column is let free in still-air conditions. Bottom graph: the column is insulated in a foam/fiber glass jacket.

the column is insulated carefully, for a compound with an apparent retention factor of about 4, under conditions such that the extra-column contributions can be neglected [65]. This demonstrates that SFC could potentially be used to accelerate analyses without losing a significant amount of resolution, provided that a meticulous insulation of the column is done and the extra-column contributions are minimized. This has been demonstrated for a column pressure drop of 25 bar and a 150 mm long column packed with 5 μm particles. A serious challenge remains, how can we operate SFC columns packed with the finer particles (1.7 μm) now available, when the pressure drop has to be about ten times larger, around 250 bar.

4.1.3. High pressures

In the previous two sections, we investigated the influence of the eluent viscosity on the speed and the resolution that can be achieved in fast liquid chromatography. Both options discussed seem to be promising, given the recent development of new thermally stable chromatographic packing materials and of practical ways (insulation) of coping with similar heat effects in columns used in SFC. For practical reasons, however, analysts may be constrained to work at room temperature (e.g., due to the chemical stability of some critical sample components) or with a certain, well defined mobile phase (e.g., for solubility or column selectivity issues).

If the column cannot be changed, the sole remaining possibility to accelerate a separation is to increase the flow rate, which means using a higher column inlet pressure. Current HPLC instruments have maximum operating pressures of 400 (Agilent 1100, 5 mL/min), 600 (Agilent RRLC, 5 mL/min), 800 (Agilent 1200, 5 mL/min), 1000 (Acquity, 1 mL/min), 1200 (Agilent 1290, 2 mL/min), and 1300 bar (Nexera, 2 mL/min). In the following discussion, the effect of the average column pressure on the viscosity of the eluent is taken into account in the estimates made of the bulk diffusion coefficients. For instance, for pure acetonitrile, a very accurate empirical relationship is provided by [40,41,66]:

$$\eta(T,P) = 10^{(A_\eta + (B_\eta/T))}\left[1 + 6.263\times 10^{-4}\left(\frac{\Delta P}{2}\right)\right] \quad (16)$$

where the temperature T and the pressure P are expressed in Kelvin and bar, respectively. $\eta(T, P)$ is given in Pa s.

The Poppe plots in Fig. 3 we derived from the HETP, $H(u_S)$, measured for naphthopyrene[2,3-a]pyrene on a 2.1 mm × 50 mm 1.7 μm BEH-C_{18} column, kept at T = 295 K under stagnant-air conditions [15], which minimizes the heat effects due to the viscous friction of the eluent stream percolating through the column bed (see Fig. 7). The minimum value of the HETP is close to 3.4 μm (e.g., $h_{min} \simeq 2.0$). This is nearly the best performance that can be achieved with sub-2 μm fully porous particles. However, as the linear velocity, hence the inlet pressure, increases, more friction heat is generated throughout the packed bed and heats it up. This heat is proportional to the power generated by the percolation of the stream, the product of the linear velocity and the pressure gradient. It is produced everywhere. It dissipates axially, along the column, and radially, across the column diameter. These dissipation causes the formation of steady axial and radial heat flux gradients. The former has a modest effect on the column efficiency. The radial thermal gradient, from the column center to the wall has a strong, negative influence on the apparent column efficiency. This radial heat flux is maintained all along the column. Because packed beds have a relatively small heat capacity (≃0.3 W/m/K), radial temperature gradients are formed, and, in turn, these gradients generate a trans-column migration velocity gradient. This explains the significant departure of the C term of columns in which significant amounts

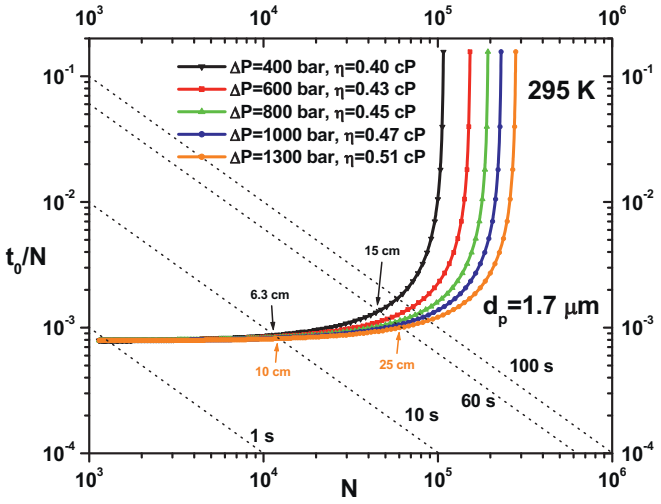

Fig. 6. Effect of the operating pressure on the Poppe plots of naphtho[2,3-a]pyrene for a column packed with 1.7 μm BEH-C_{18}. Note how insignificant is the effect of using a very high pressure in fast chromatography when the hold-up time is smaller than 20 s.

of heat are generated toward higher values with increasing mobile phase velocity.

The effects of an increase of the accepted pressure drop on the Poppe plots are illustrated in Fig. 6. However, the contributions to band broadening of the instruments (Agilent 1100, Agilent 1290, Nexera, etc.) were not taken into account in these plots. Remarkably, the higher the maximum pressure at which the experiment is performed, the larger the maximum column efficiency that can be expected at very low velocities, with infinitely long columns. This confirms the prediction implied in Eq. (15) that the limit efficiency is directly proportional to $\Delta P/\eta$. Consequently, the advantages brought by vHPLC instruments are most useful in the range of the large hold-up times, at least in excess of a minute. In contrast, there is virtually no interest in applying very high inlet pressures in fast liquid chromatography, for hold-up times equal or smaller than 10 s. The explanation lies in the steep increase of the HETP of retained compounds with increasing linear velocity. The possible gain in analysis time is balanced by the loss in column efficiency due to the mass transfer resistance and to the thermal effects.

In conclusion, this section demonstrates that an increase of the operating pressure alone is not a really good solution to achieve

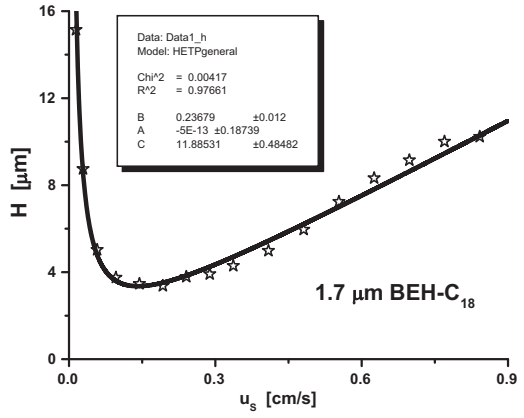

Fig. 7. Experimental HETP data measured for naphtho[2,3-a]pyrene on a 2.1 mm × 50 mm 1.7 μm BEH-C_{18} column eluted with pure acetonitrile. T = 295 K. The column is left in stagnant-air conditions. Note the steep C term due to frictional heating and the associated trans-column band dispersion at high velocity.

very fast separations with hold-up times smaller than a few tens of seconds. The use of high column inlet pressures is merely the price to pay for operating columns packed with fine particles.

4.1.4. High permeability column: monolithic columns

Faster analyses could be obtained by using high permeability columns, provided that they can provide a satisfactory efficiency. In the 1970s, Huber tried to loosely pack columns to increase their permeability. It turned out that the few high-permeability columns that he could produce were short-lived because their mechanical stability was poor and the approach was abandoned [67]. Around the turn of the millennium, a new type of stationary phase with a high permeability was developed by Tanaka and Nakanishi [6]. In the same times, other scientists developed columns made of porous blocks of polymers. These so-called monolithic columns are made of a single block having a bimodal pore size distribution. Interestingly, the size of the small pores (the mesopores responsible for the retention of the analytes) and that of the large pores (the throughpores responsible for the percolation of the mobile phase and the permeability of the monolithic structure) can be adjusted independently. The average size of the throughpores is usually around 2 μm, leading to a column permeability around 8×10^{-14} m^2, which is comparable to that of columns packed with 11 μm spherical particles [8]. In addition, the minimum plate height of these monolithic columns is comparable to that of columns packed with 5 μm particles. Fig. 8 shows the plate heights of the 5 μm Luna-C_{18}(2) packed columns and Onyx-C_{18} monolithic columns.

Depending on the chemical nature of the monolith selected, on its surface chemistry and on the type of chemical groups bonded to its surface, on the mobile phase and on the other experimental conditions selected, the use of monolithic columns may offer one or several advantages. These columns are easier to prepare in the laboratories of those who have mastered the synthetic procedure (essentially the polymeric columns). They are easier to use for the separations of very large solutes such as antibodies and even viruses, due to their large through-pores and to the fast convection that brings solutes to the surfaces of these pores, provide fast separations, and have modest requirement for high pressure pumps.

The comparison between the two HETP curves in Fig. 8 reveals that the Cu_S term of the monolithic column is not as flat as it could have been expected, given the small size of the interconnected porous skeleton elements (≃1 μm). Actually, this slope is slightly steeper than that of the column packed with 5 μm particles. A recent investigation of the mass transfer mechanism in monolithic columns [9] demonstrated that the source of this problem is not in the solid–liquid mass transfer resistance, which is usually faster than in packed columns, but is due to a significant long-range velocity bias in these monolithic silica rods. Peaks tail significantly at high flow rates. The derivation of the column efficiencies from the values of the first and second moments calculated by numerical integration affects the Poppe plot of monolithic columns. When the column is operated at high velocities, this tailing reduces the resolution and the plate number of the column. As shown in Fig. 9, the advantage of monolithic columns over columns packed with 5 μm particles is obvious only when the analysis time is larger than about 30 s that is when the HETP is mostly controlled by longitudinal diffusion. According to Eq. (15), the maximum efficiency that can be achieved is proportional to the permeability, two to three times larger for the Onyx than for the Luna-C_{18}(2) column. In contrast, in fast chromatographic analysis, the slope of the C branch of the HETP plot is critical. For elution times around 10 s, the gain in permeability is compensated by the loss in column efficiency caused by the important trans-column velocity biases. Fig. 10 shows that at superficial linear velocities larger than 0.15 cm/s (or at flow rates larger than 1.5 mL/min with a 4.6 mm I.D. monolithic column), the eddy

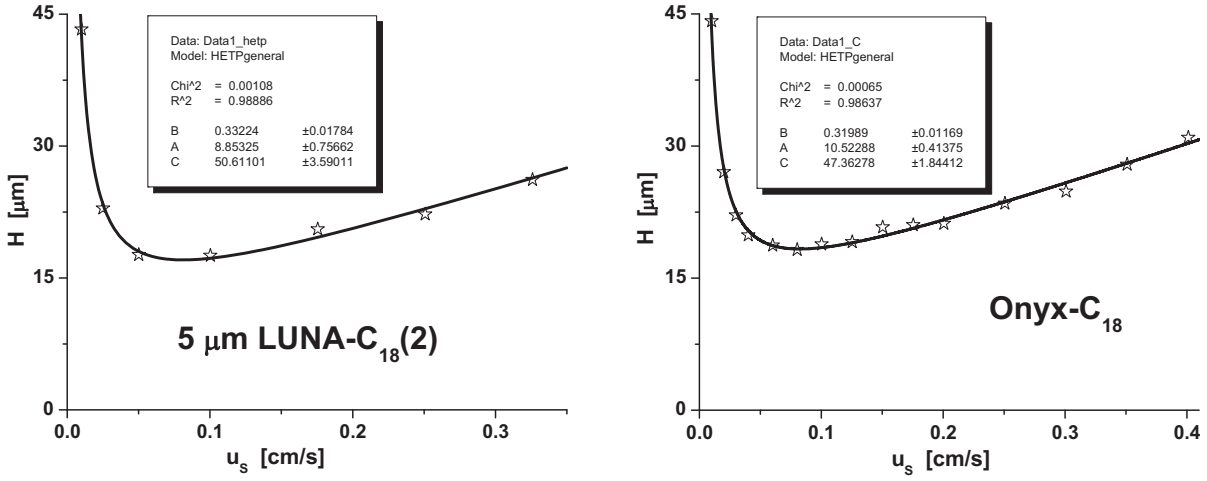

Fig. 8. Comparison between the experimental HETPs of columns packed with 5 μm particles and of silica monolithic columns. Left graph: 5 μm Luna-C_{18}(2) packed column, phenol, methanol/water, 10/90, v/v, T = 295 K. Right graph: Onyx-C_{18} monolithic column, naphthalene, acetonitrile/water, 55/45, v/v, T = 295 K. Note the equivalent performance of both columns.

dispersion term penalizes severely the resolution of the separation because it accounts for at least 90% of the total band dispersion and it steadily increases with increasing flow rate. The eddy diffusion term increases due to significant transcolumn or at least long-range velocity biases. The range of linear velocities applied is not large enough to observe a constant flow-controlled dispersion mechanism. Therefore, the radial concentration gradients are partially relaxed by radial dispersion of the sample molecules and the eddy diffusion term follows the coupling mechanism between a flow-controlled and Aris-Taylor diffusion-controlled eddy dispersion. Overall, regarding applications in fast liquid chromatography, we regret to observe that current monolithic columns perform barely as well as conventional columns packed with 5 μm particles.

The reason for the mediocre performance of monolithic columns is the radial heterogeneity of the silica rods and the important unevenness of the radial distribution of the mobile phase velocity across these columns. Hopefully, new synthesis procedures will some day produce more radially homogeneous monolithic structures and the columns made with these new rods will be fitted to a sample distributor of improved design. Otherwise, these columns will keep playing an insignificant role in the realm of practical applications of HPLC.

4.1.5. High efficient columns packed with sub-2 μm particles

Fast, high-resolution chromatography is now attempted and often achieved with columns packed with sub-2 μm particles. These columns may provide minimum plate heights as small as 3.5 μm or nearly a four times smaller than those observed with conventional columns packed with 5 μm particles or with monolithic columns. To cope with the low permeabilities of columns packed with 1.7 μm particles ($k_0 \simeq 2.5 \times 10^{-15}$ m^2), which are between thirty and ten times smaller than those of monolithic columns and of packed (5 μm particles) columns, respectively, pumps able to provide streams of solvent under very high pressures are necessary.

Fig. 11 illustrates the theoretical advantage of operating with smaller particles at a constant pressure of 400 bar. Note that because the column permeability decreases with decreasing particle size, the maximum column efficiency drops from about 200 000

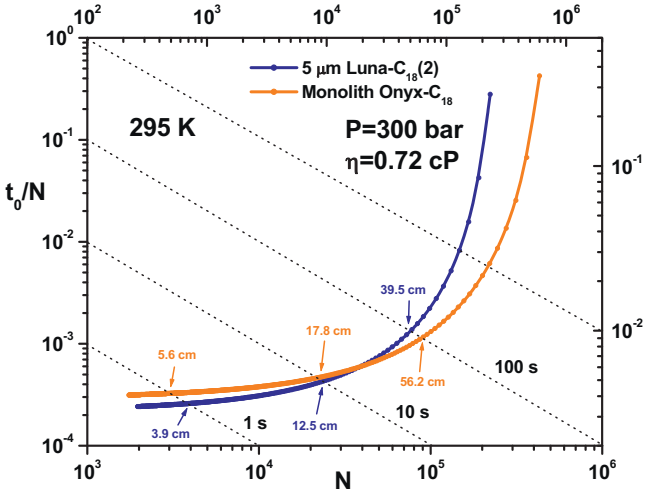

Fig. 9. Comparison between the Poppe plots of a monolithic (4.6 mm I.D.) and a packed (5 μm particles) column. Note their equivalent performance in fast chromatography.

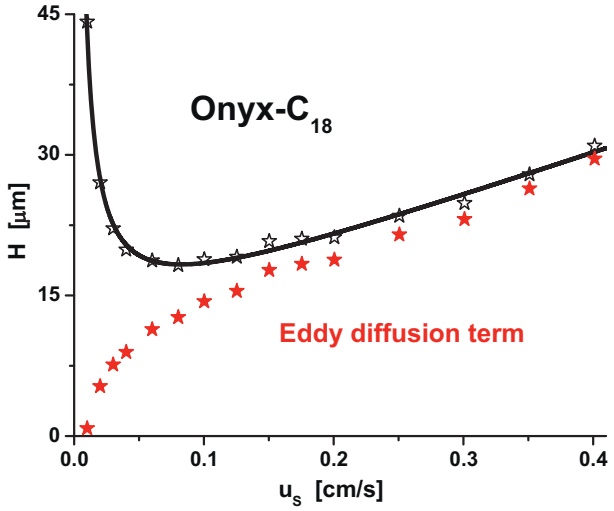

Fig. 10. Experimental HETP of a monolithic column (4.6 mm I.D.). Sample: naphthalene. Eluent: acetonitrile/water, 55/45, v/v. T = 295 K. The black solid line represents the best adjusted van Deemter curve. The red stars show the contribution of the eddy dispersion term, which accounts for more than 90% of the total HETP at high flow rates. (For interpretation of the references to color in this figure legend, the reader is referred to the web version of the article.)

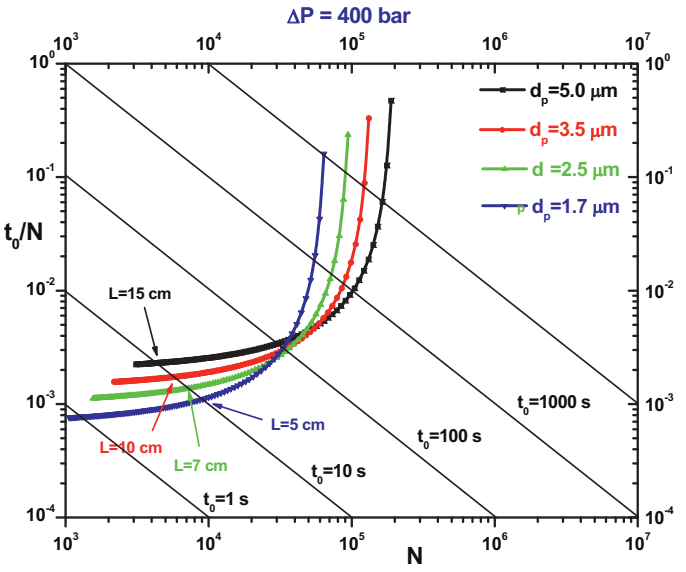

Fig. 11. Impact of the particle size of the packing material on the Poppe plots of packed columns. Note the advantage offered by small particles in fast chromatography.

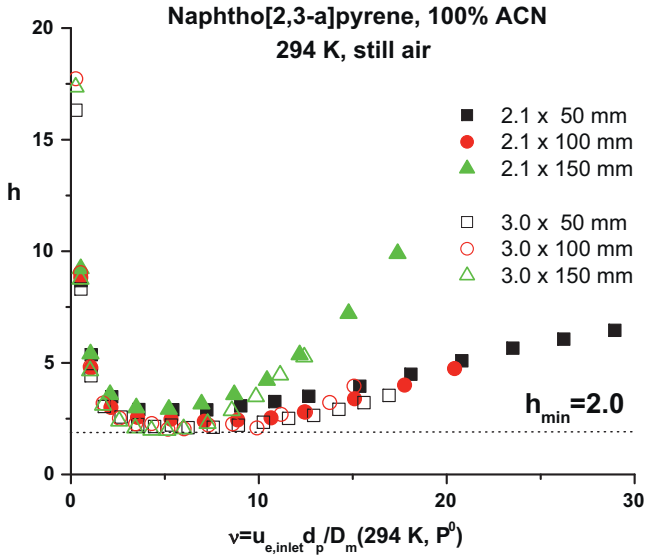

Fig. 12. Influence of the heat friction on the efficiency of columns packed with sub-2 μm particles. The columns is under stagnant-air environment. Note the deviation of the actual HETP curve with respect to the expected HETP, would the temperature of the bed be uniform.

to 70 000 plates in the upper right corner of the graph. Most importantly, however, small particles provide excellent performance for hold-up times smaller than a minute. This conclusion holds true as long as frictional heating effects do not have to be taken into account in the expression of the plate height, as shown in Fig. 11. This approximation does remain reasonable for inlet pressures below 400 bar. In this case, the HETP plot becomes flatter at high velocity and the benefit of using smaller particles is clearly visible. For instance, a hold-up time of only 10 s could be achieved with 15 cm long columns packed with 5 μm particles and with a three times shorter column packed with 1.7 μm particles. Eventually, the gain in resolution would then be two-folds.

However, columns packed with sub-2 μm particles are often used with higher inlet pressures, up to 1000–1300 bar and high velocity streams flowing under high pressure gradients generate frictional heat. Therefore, as shown in Fig. 7, the *C* branch of the HETP curve is not as flat as it was theoretically predicted for the hypothetical isothermal column. Fig. 12 illustrates the actual loss in column efficiency for column of different dimensions (2.1 and 3.0 mm I.D., 5, 10, and 15 cm long). The longer the column, the larger the plate height increase because radial temperature gradients are fully developed and take place along a significant fraction of the column length. This explains the origin of the parabolic shape of the *C* branch of those long columns. With shorter columns, the radial temperature gradients are only partially developed and the overall *C* branches remain nearly linear but with a slope markedly steeper than theoretically expected.

As a result, it would be better to perform fast liquid chromatography at high temperatures, since the column back pressure might be decreased, hence the amount of heat generated in the column would be lower, and this would improve the resolution power. The downside of this approach is the necessary presence of an eluent preheater, which could affect the efficiency of the least retained peaks under isocratic conditions.

A major issue with the use of short columns packed with sub-2 μm particles in fast chromatography is that the contribution of the extra-column volumes of the chromatographic instrument to the broadening of eluted bands might impose strict limitations to attempts at decreasing the column dimensions beyond certain limits. The volume contribution of the instrument to the measured width of eluted bands must be relatively small compared to that of the column, $\sigma^2_{v,\text{column}}$, which is given by [32]:

$$\sigma^2_{v,\text{column}} = \frac{V_0^2}{N}(1+k)^2 \quad (17)$$

otherwise, the actual resolution power of the column is degraded and a reduced part is actually available.

As an example, consider the elution of a retained compound with $k = 1$ on a 50 mm × 2.1 mm column packed with fully porous sub-2 μm BEH particles, which has a HETP of 4 μm. The total porosity is $\epsilon_t = 0.65$, so $V_0 = 113$ μL, $N = 12\,500$, and $\sigma^2_{v,\text{column}} = 4\,\mu\text{L}^2$. Unfortunately, the peak variance contribution of the best available standard vHPLC instruments is between 5 and 10 μL^2 [32,65,68]. This limits the possibility of successfully using such a column to perform isocratic separations. In other words, in the best of cases, the apparent efficiency of the narrow-bore column taken as example would be at best twice to thrice smaller than the true column efficiency. Admittedly, the performance achieved for separations made under gradient elution will be better since then only the extra-column volumes in the downstream part of the instrument (connection to the detector, detector cell volume, and data acquisition rate) contribute to band broadening because the sample band is concentrated at the column inlet. This issue is critical in fast chromatography because the extra-column variance of the instrument increases with increasing mobile phase velocity [65]. Under isocratic conditions, no more than 40% of the full intrinsic efficiency of the column can be observed with moderately retained compounds. More conventional instruments of the previous generation operate at an inlet pressure of only 400 bar and contribute by ca. 40 μL^2 to the variance of eluted peaks. They are useless to operate modern columns.

The solutions to this problem are mainly practical : the inner diameter of the connecting tubes should be shrunk to about 100 μm, the detection cell volume should be no larger than 1 μL, and the injection system design should be such that, during its transfer to the column inlet, the sample do not flow through the injection valve and its needle seat capillary. Also the instrument design should minimize the lengths of the connecting tubes from injector to column inlet and from column outlet to detector. This will limit the flow resistance of the thin capillary tubes. Otherwise,

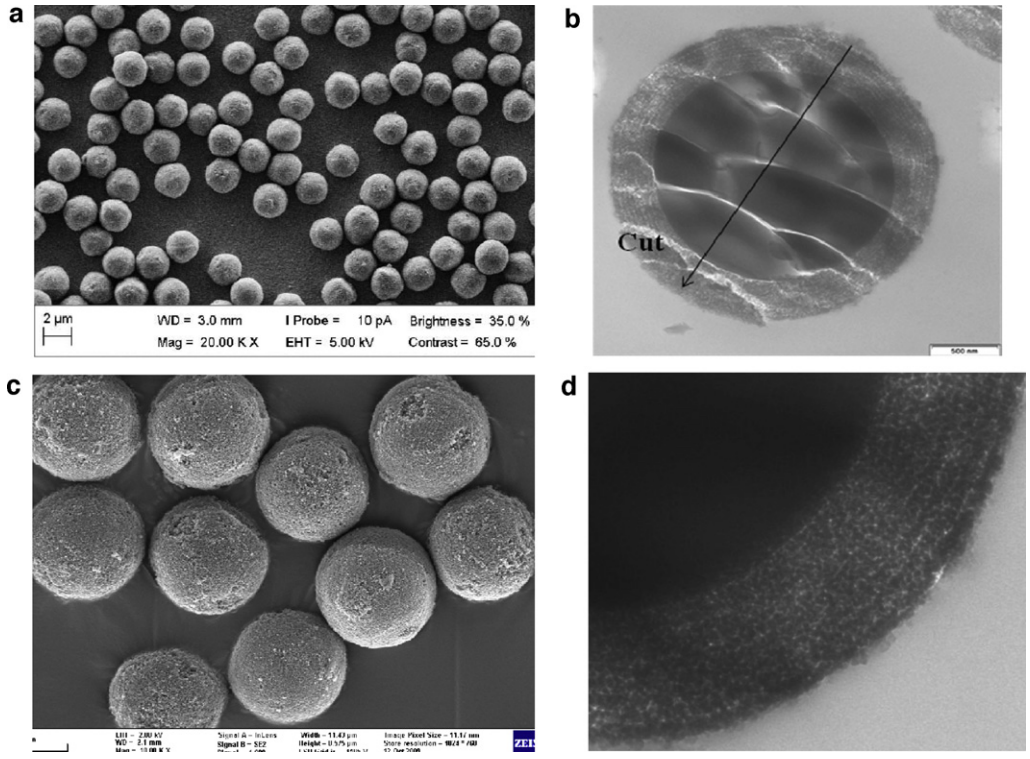

Fig. 13. SEM pictures of the 2.6 Kinetex shell particles (Phenomenex, Torrance, CA, USA). The right pictures show particle cuts.

analysts might be constrained to operate at flow rates lower than optima, which decreases the speed of analyses.

4.1.6. Permeable and highly efficient columns: sub-3 μm shell particles

The recent development of columns packed with sub-3 μm shell particles offers an attractive alternative to the use of monolithic columns (high permeability) or even columns packed with sub-2 μm particles (high efficiency and short columns). Shell particles are made of a solid core surrounded by a layer-like structured porous shell obtained by a step-by-step growth process around the core. Fig. 13 shows scanning electron microscopy photographs of commercial shell particles. The commercial particles have a narrow size distribution, with a relative standard deviation (5%) much lower than that (15–20 %) of conventional fully porous particles (top left graph). The external surface of these particles is irregular and rough (bottom left graph), much rougher than that of fully porous particles, as previously discussed [26]. The relative thickness of the porous shell is such that the volume fraction of the porous shell of the 2.6 μm Kinetex particles is around 60%, providing this material a sufficiently large specific surface area (top right graph). Their sample loading capacity is comparable to those of fully porous particles, eliminating the drawback of the earlier generations of shell particles, for which the porous shell accounted for only 10% of the total particle volume [27].

Because their particles are larger, the permeability of columns packed with shell particles is larger, two to three times larger, than that of columns packed with sub-2 μm particles ($k_0 = 6$ rather than 2.5×10^{-15} m^2). As a result, these columns can be operated with a lower inlet pressure, which generates a lower amount of heat due to heat friction. Their HETPs increase more slowly with increasing flow rate than those packed with fully porous particles. Remarkably, the minimum plate height of these columns is comparable with those of columns packed with sub-2 μm, with $H_{min} \simeq 3.5$ μm [24,25]. The reason is their lower longitudinal diffusion coefficients, B (−15 to −30% depending on the retention factor in RPLC), and eddy diffusion terms, A (−40%). Surprisingly, the impact of a reduction of the B coefficient is far from negligible in fast chromatography, although the longitudinal diffusion HETP term is inversely proportional to the eluent linear velocity. Actually, most of the exceptional performance of 4.6 mm I.D. columns packed with sub-3 μm shell particles is due to a low rate of dispersion in the interstitial mobile phase.

The low eddy diffusion term of columns packed with shell particles is not due to lower contributions of the trans-channel and short-range inter-channel eddy diffusion terms [26,52,69] nor to the tighter particle size distribution of shell particles (5% *versus* 15%). It seems better explained by the significant reduction of the trans-column and/or long-range inter-channel velocity biases. This is probably due to the better structure of the packed beds obtained. The roughness of the surface of the sub-3 μm shell particles causes strong friction between them and between the bed and the column wall. During the consolidation of the bed under the very high compression pressure applied, the shear friction forces between these particles are strong enough to prevent their relative motion. In contrast to the smooth fully porous particles, they poorly slip by respect to their neighbor. The result is that the stress distribution remains wider in beds of shell particles while the strain distribution is narrower than in beds of fully porous particles. This explanation is consistent with the values measured for the average external porosity of columns, around 0.40 for shell particles instead of 0.35–0.37 for the smooth fully porous particles. Then, the strain differential between the bed regions near the wall (high stress) and the center of the column (low stress) being lesser, the radial distribution of the external porosity is more homogeneous, resulting in a more homogeneous distribution of the axial velocities across the column. This is also consistent with the measures made by local electrochemical detection showing that the trans-column velocity bias in columns packed with 2.7 μm Halo [26] and 2.6 μm Kinetex [70] shell particles is significantly reduced compared to fully porous particles.

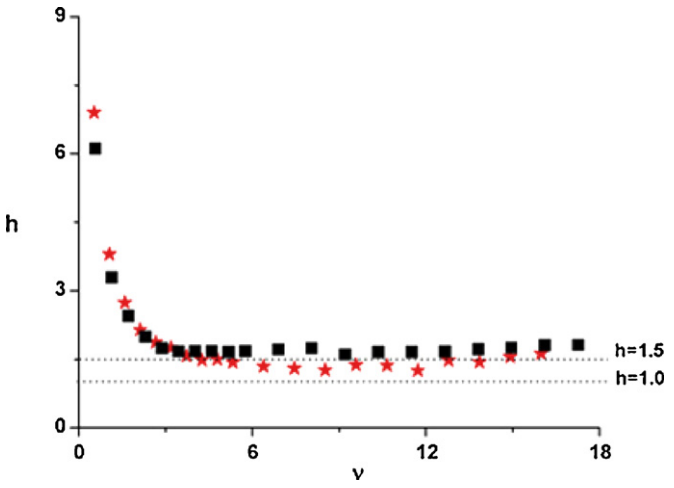

Fig. 14. Reduced plate height of naphtho[2,3-a]pyrene measured at 295 K with pure acetonitrile on 4.6 mm I.D. columns packed with 2.6 μm Kinetex-C_{18} (full red star symbols) and 2.7 μm Halo-C_{18} (full black square symbols) shell particles. (For interpretation of the references to color in this figure legend, the reader is referred to the web version of the article.)

Fig. 14 shows the reduced HETPs of 4.6 mm I.D. columns packed with 2.6 μm Kinetex and 2.7 μm Halo shell particles. The minimum reduced HETPs of these columns are between 1.2 and 1.5. Fig. 15 compares the performance of a 4.6 mm I.D. monolithic column (Onyx-C_{18}) at 300 bar, of a 2.1 mm I.D. column packed with sub-2 μm particles (1.7 μm BEH-C_{18}) at 1000 bar, and of a 4.6 mm I.D. column packed with shell particles (2.7 μm Halo-C_{18}) at 400 bar. Clearly, the first generation of 4.6 mm I.D. monolithic columns are no longer competitive with columns packed with modern sub-2 μm fully porous particles or sub-3 μm shell particles. The advantage of the shell particles over the fully porous ones is also clear. They combine a higher permeability (6×10^{-15} m^2) with an exceptionally low plate height ($H_{min} \simeq 3.5$ μm). Furthermore, this lower HETP value is observed in the whole range of large linear velocities that is accessible. As a result, with a pressure drop of only 400 bar, smaller analysis times (at constant column efficiency) and larger efficiencies (at constant analysis time) can be generated with columns packed with shell particles than with those packed with sub-2 μm particles operated at a larger inlet pressure of 1000 bar. However, we must emphasize that this performance can only be

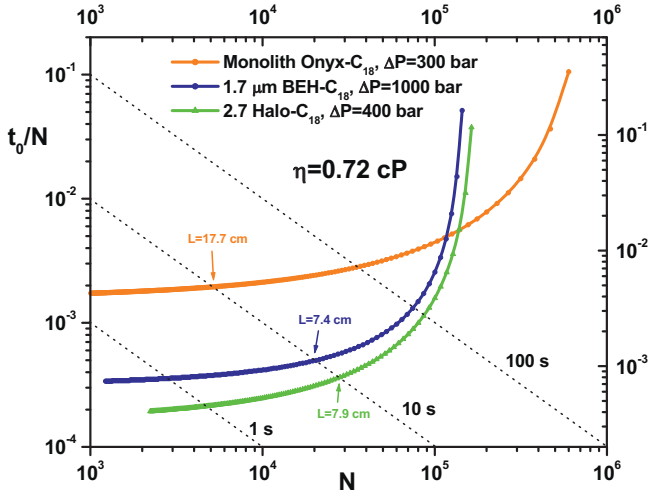

Fig. 15. Comparison between the Poppe plots of 4.6 mm I.D. monolithic column, 2.1 mm I.D. columns packed with sub-2 μm particles, and 4.6 mm I.D. columns packed with sub-3 μm shell particles.

achieved if the extra-column band broadening contributions of the standard 400 bar instruments can be minimized and decreased to values as low as those observed with vHPLC instruments. The peak variance of these vHPLC instruments at high flow rates is typically around 10 μL^2.

4.2. Current ultimate speed achievable in 1D HPLC

In this section, we assess from a qualitative point of view the performance of the fastest and most efficient 1D HPLC separation method that can be achieved with the columns and instruments currently available.

The role of the mobile phase is critical in fast elution chromatography and the properties of solvents available should be carefully considered. In both the RPLC or the HILIC mode, the use of mixtures of acetonitrile and water is preferred because their viscosity is lower than that of all the alcohol/water mixtures. It is also recommended to always consider whether it is possible to operate the column at a somewhat higher temperature than initially considered and to check the thermal stability of the sample components and of the columns considered because this would allow a further decrease of the eluent viscosity and faster analyses. In the following, we will consider a mobile phase made of a water/acetonitrile (40/60) mixture, at 60 °C; its viscosity is 0.27 cP under atmospheric pressure.

To further accelerate a separation, whatever the required column efficiency, the use of an instrument allowing the use of very high inlet pressures is necessary. So, we will operate the column at a constant pressure of 1000 bar. Several instruments permit now the use of higher pressure but modern instruments have a significant contribution to the column back pressure, due to the hydraulic resistance of their tubings. Because the viscosity of liquids increases with increasing pressure and does so linearly [39], the average viscosity of the eluent is the viscosity at the average column pressure (500 bar), 0.35 cP (see Eq. (16)).

The best columns now have a very low HETP that should not increase rapidly with increasing mobile phase velocity, due to the generation of excessive heat by friction of the eluent against the bed. The columns packed with 1.7 μm core–shell particles provide a very low Cu_S term because the thermal conductivity of their bed immersed in a water/acetonitrile mixture is high (0.60 W/m/K), higher than that of the columns packed with fully porous BEH particles [71,72]. This limits the amplitude of the radial temperature gradient formed across the column [30,31]. In addition, due to the size of these sub-2 μm shell particles, the column HETP is around 3.5 μm over a wide range of high linear velocities. Fig. 16 shows the HETP of a 150 mm × 2.1 mm column packed with 1.7 μm Kinetex-C_{18} shell particles measured for naphtho[2,3-a]pyrene in pure acetonitrile at 295 K. The striking feature is the very flat Cu_S branch of the HETP curve, compared to the slope of the same curve for a 50 mm × 2.1 mm column packed with 1.7 μm fully porous BEH-C_{18} particles in Fig. 7.

Finally, it is not practical to operate under isocratic conditions columns shorter than 5 cm, due to the size of the band broadening contribution of the instruments currently available. Therefore, we can reasonably select a $L = 5$ cm as the shortest available column length. The analysis of the Poppe plot at a constant inlet pressure of 1000 bar, with an eluent of viscosity 0.35 cP predicts a hold-up time $t_0 = 1.5$ s and a column efficiency of 4760 plates. The corresponding superficial linear velocity is 1.71 cm/s or an interstitial linear velocity of 4.2 cm/s. The reduced interstitial linear velocity is then $\nu = ud_p/D_m \simeq 35$ for naphtho[2,3-a]pyrene ($D_m \simeq 2 \times 10^{-5}$ cm^2/s), a value clearly larger than the optimum reduced velocity, $\nu_{opt} = 10$ to 15. The HETP expected at such a high linear velocity is 10.5 μm, a value three times larger than the minimum plate height (3.5 μm). The expected flow rate for a 2.1 mm I.D. column would then be

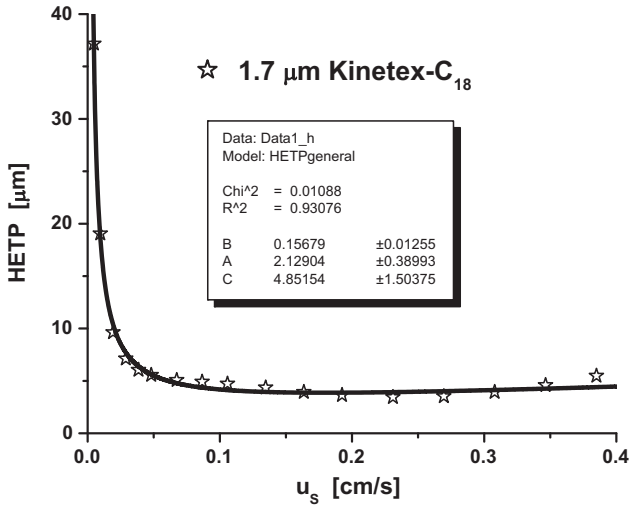

Fig. 16. HETP of a 150 mm × 2.1 mm column packed with 1.7 μm Kinetex-C_{18} shell particles, measured for naphtho[2,3-a]pyrene eluted with pure acetonitrile. The permeability of this column was $k_0 = 3.0 \times 10^{-15}$ m^2 [31].

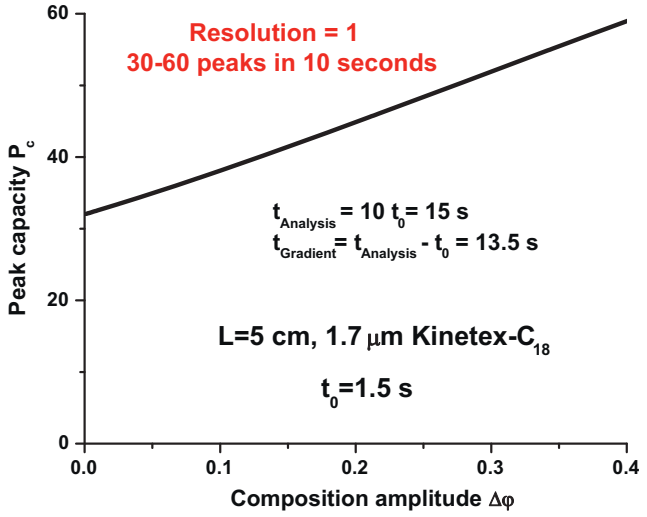

Fig. 17. Estimate of the peak capacity expected under gradient elution conditions using a 2.1 mm × 50 mm column packed with 1.7 μm Kinetex-C_{18} particles, run at a flow rate of 4.1 mL/min and at a maximum pressure drop of 1000 bar. The eluent is a mixture of acetonitrile and water (60/40, v/v) heated at a temperature of 60 °C.

$1.71 \times \pi \times 0.105^2 \times 60 = 3.55$ mL/min. The highest flow rates that current vHPLC systems can deliver at 1000 bar are 1 mL/min, 3.5 mL/min, and 4.1 mL/min for the Acquity, the 1290 Infinity, and the Nexera systems, respectively. Both the 1290 Infinity and Nexera instruments could operate at such a high flow rate and at a pressure of 1000 bar. The Acquity system could not.

In conclusion, it is possible to generate today hold-up times t_0 of only 1.5 s with short 50 mm × 2.1 mm columns that would eventually have a true efficiency of 4760 plates. If the band broadening contribution of the vHPLC system is minimized by using a 800 nL detector cell volume, connecting tubes and needle seat capillary with an I.D. of 115 μm, and an injection volume of 0.2 μL, the instrument's contribution could be as small as 7 μL^2 at a flow rate of 4.0 mL/min [65]. According to Eq. (17), the variance contribution of the band eluted from this 2.1 mm × 50 mm column for a moderate retention factor $k = 1$ would be 7.5 μL^2. Accordingly, under isocratic conditions, the recorded chromatogram would show an apparent efficiency of 2460 plates, for an analysis time of 3.0 s.

Under gradient elution conditions, the band broadening contribution of the vHPLC system is less important because the sample is concentrated at the column inlet. It is essentially limited to the part due to the extra-column volume downstream the column. It was recently observed that the influence of the detection cell volume on the total extra-column band broadening is particularly important at very high flow velocity [65]. For instance, with a flow rate of 4.0 mL/min, a connecting tube I.D. of 115 μm and an injection volume of 0.20 μL, the extra-column peak variance increases more than twice, from 7 μL^2 to 17 μL^2 when the volume of the detector cell increases from 0.8 to 2.4 μL. A simple, approximate extrapolation to a zero volume detector cell suggests that the extra-column peak variances due to the injection system and the needle seat capillary would be only around 2 μL^2. Therefore, the contribution of the 800 nL detection cell is most likely around 5 μL^2 and the apparent column efficiency expected under gradient elution would be that of 2860 plates column, assuming that band compression during the gradient elution is negligible and the elution time of the sample is twice the hold-up time.

An account of the band compression factor of a compound is theoretically possible [73] when its retention behavior obeys the Linear Strength Model (LSM) model [74] defined by the retention slope, S. It was recently demonstrated that the exact peak capacity is written [25]:

$$P_c = 1 + \frac{1}{4}\sqrt{\frac{3N}{\omega}}\ln\left[\frac{2\kappa e^{Gk_F} + G^2 - 6 + \psi}{G\left(2\sqrt{3\kappa} + 3G + 6\right)}\right] \quad (18)$$

where

$$\kappa = G^2 + 3G + 3 \quad (19)$$

$$\psi = 2\sqrt{\kappa[(G^2-6)e^{Gk_F} + \kappa e^{2Gk_F} + G^2 - 3G + 3]} \quad (20)$$

$$k_F = \frac{t_F - t_0}{t_0} \quad (21)$$

where t_F is the gradient elution time of the last eluted compound and G is the intrinsic gradient steepness which is written [75]:

$$G = S\beta t_0 \quad (22)$$

and where β is the gradient steepness ($\Delta\varphi/t_G$). $\Delta\varphi$ is the amplitude of the volume fraction of the strong eluent from the start to the end of the gradient.

Fig. 17 shows the expected maximum number of peaks resolved or peak capacity for a peak resolution of 1, with $k_F = 9$ (the analysis time is equal to 15 s), and $S = 10$ (small molecules) as a function of the change in the mobile phase composition from start to finish. It is remarkable that such a column could still potentially resolve about 40 peaks for a physically possible gradients, easily compatible with current vHPLC instruments. The increase of the strong eluent concentration by 20% within 13.5 s can be carried out accurately and precisely given the robustness of the eluent mixer and the very small dwell volume between the mixer and the column inlet.

4.3. How much faster could 1D HPLC become in the new decade?

Most possible means of accelerating further chromatographic separations have been nearly exhausted. Pursuing classical methods is now hitting new roadblocks that seem difficult to overcome. The most promising possibilities still available at this stage are (1) the development of packing materials that are stable at high temperatures, in the 150–200 °C range or even higher; some progress is already being achieved in this direction [76,77]; (2) the production of advanced monolithic columns, which would provide efficiencies comparable to those of columns packed with the finer

particles available today. There has been rumors of progress being made in this area for a long time but serious difficulties seem to remain unsolved. A successful second-generation monolithic column should be far more radially homogeneous and have an average domain size smaller than the first-generation ones; and (3) the preparation of smaller shell or fully porous particles which could be packed into shorter columns. This approach might appear to many as the most promising one, since it continues a fifty-year-old trend which has consistently proven highly successful to reduce analysis times; yet it is hindered by overwhelming physical limitations. Three serious obstacles can be identified on this way, for which solutions or palliatives are now discussed.

1. Because shell particles pack so much better than fully porous particles, it seems that any attempt at preparing and using finer particles should use this same model. Because the sources of band broadening originating from axial and eddy dispersion are relatively less important in columns packed with shell than with fully porous particles, the optimum reduced interstitial velocity in these columns is usually of the order of 10 instead of around 5–6, as it is for columns packed with fully porous particles. A direct extrapolation to 1 μm particles suggest that the optimum interstitial linear velocity of columns packed with them would be:

$$u_{opt} = \frac{10 D_m}{d_p} \tag{23}$$

If we consider the separation of small molecules and assume $D_m = 2 \times 10^{-5}$ cm^2/s for compounds with a molecular weight of 100–300 g/mol, the optimum interstitial linear velocity for columns packed with 1 μm particles can be estimated at 2 cm/s. With 2.1 mm I.D. columns, the flow rate would be around 1.7 mL/min, which is still in the range of what today vHPLC instruments can supply. Obviously, 4.6 mm I.D. should not be considered. The optimum flow rate for these columns would be around 8.5 mL/min. We show below that heat effects in such columns would result in unacceptable performance.

The column permeability being proportional to d_p^2, we can reasonably expect for these columns $k_0 = 9 \times 10^{-16}$ m^2. The inlet pressure required to percolate a 5 cm long column eluted with water (viscosity 1 cP) at the flow velocity of 2 cm/s, would be 4.5 kbar. Only a new generation of ultra-high pressure instruments could operate columns at such extremely high pressures. Admittedly, capillary columns were operated at 7 kbar, under micro-flow conditions [78–81]. Since current instruments cannot deliver eluent streams at pressures larger than 1.3 kbar with flow rates larger than 2 mL/min, the alternatives would be to use three times shorter columns or a less viscous eluent, e.g., at elevated temperature ($\eta = 0.10$ cP). Then, the inlet pressure would drop down to about 1.3 kbar, a value still acceptable for the currently available vHPLC instruments, albeit at the very limit of their capability. Besides, the band broadening of current instruments would be unacceptably large for these columns. Only a radical change in the very design of instruments and their miniaturization would be necessary.

2. The second problem is related to the amplitude, ΔT of the radial temperature gradients and their nefarious effect on band broadening [14,15,41,42,82]. Under controlled wall temperature (for instance by immersion of the chromatographic column in a liquid bath), the amplitude of this temperature gradient is written [83]:

$$\Delta T = (1 + \alpha_p T) \frac{u_S r_c^2 \Delta P}{4 \lambda_p L} \tag{24}$$

where α_p is the thermal expansion coefficient of the eluent. For liquids, $\alpha_p T \simeq -1/3$ [39]. This constraint is not optimum.

Today, it is still possible to minimize the impact of these radial temperature gradients with sub-2 μm core–shell particles by selecting thermal environment conditions close to the ideal adiabatic condition (for instances, by placing the column in still-air environment or by cladding it with a thermally insulating material) even when the pressure drop is as high as 1.3 kbar. First, the I.D. of the columns should be kept small such as with narrow-bore columns (2.1 or even 1 mm). Secondly, the effective heat conductivity of the packed bed of shell particles immersed in an acetonitrile/water mixture (60/40, v/v) is of the order of 0.60 W/m/K. Accordingly, when fully developed, the amplitude of the radial temperature gradient across a 2.1 mm I.D. column packed with 1.7 μm particles at the optimal superficial linear velocity of 1.2 cm/s is about 10 K. With 1 μm particle size, if the optimum linear velocity is increased to 2 cm/s, the pressure drop reaches 3.8 kbar, and the amplitude of the radial temperature gradient is multiplied by $1.7^3 \simeq 5$. We then expect extremely high radial temperature gradients up to 50 K along a short distance of only 1.05 mm.

Accordingly, assuming that we dispose of high pressure pumps operating up to 4 kbar, this exponential increase of the radial temperature gradients by a factor 5 when the size of the particle decreases by a factor 1.7 could be compensated in two different ways. First, the inner diameter of the column could be decreased by a factor $\sqrt{5}$, e.g. one should use column with an inner diameter of 1 mm. Alternately, the effective thermal conductivity of the packed bed should increase by a factor 5. One simple way would consist in replacing the non-porous silica cores with non-porous alumina ($\lambda_{AlO_2} = 40$ W/m/K) or gold ($\lambda_{Au} = 320$ W/m/K) cores [72]. According to the Zarichniak's expression, which predicts the thermal conductivity of randomly distributed binary composite materials [84], the thermal conductivity of the packed beds made with these new core–shell particles would increase from 0.6 to 2.32 (×4) and 12.5 (×21) W/m/K. In fact, the thermal conductivity of the new non-porous cores should be around 60 W/m/K which will allow the analysts to operate 2.1 mm I.D. narrow-bore columns and drastically reduce the influence of the heat effects on the column efficiency. The heat generated by friction will dissipate in the same way as for columns packed with silica based materials but at a much faster rate due to the larger thermal conductivities of these materials being larger than that of neat silica (1.4 W/m/K). The physical consequence is a diminution of the amplitude of the radial temperature gradients as shown in Eq. (24).

3. The third problem is related to the extra-column contribution of the next generation of micro-HPLC systems to the peak variance. Anticipating an intrinsic optimum reduced plate height of 4 with a 1.0 mm × 50 mm columns packed with 1 μm particles ($N = 12\,500$) because we can predict a lower reduced plate height with finer particles packed into narrower tubes, the peak variance of such column for a moderately retained compound ($k = 1$) would be around 0.2 μL^2. Accordingly, it is absolutely necessary that the extra-column band broadening of these new micro-HPLC systems be smaller than 0.1 μL^2 in order to conserve about 50% of the intrinsic column efficiency. This will require a new instrument design.

4.4. Importance of capillary columns in fast LC?

In this last section, we briefly discuss the potential role of packed capillary columns in pressure- driven fast liquid chromatography. The obvious advantage of capillary columns is the practical absence of additional band broadening due to frictional heating due to the use of very small nano-flow rates. The inner diameter of these columns typically varies between 10 and 300 μm [78]. Therefore, assuming a retention factor $k = 3$, a column 50 mm long, packed with

1 μm shell particles, providing a minimum reduced plate height $h_{min} = 3$, the column variance would be between 3.7 nL^2 (10 μm I.D. capillary) and 0.003 μL^2 (300 μm I.D. capillary). Consequently, current standard μ-HPLC systems operating at a maximum pressure drop of 800 bar, equipped with a 6 position/2 ports injection valve and a post-column detector would be inappropriate to run such columns due to the pressure limitation and the excessively large extra-column band variance caused by the injection valve (≃50 nL), the detection cell (≃100 nL), and the 25 μm I.D. connecting tubes (≃50 nL), combination of extra-column volumes that already gives a variance contribution as high as 0.010 μL^2[85]. Additionally, the band spreading due to column/tubes connections can significantly increase the system band broadening. High performance capillary endfittings are required to support the very high pressure of about 4 kbar that are expected at the optimum linear velocity required with small molecules ($D_m = 1.5 \times 10^{-5}$ cm^2/s) and a low-viscosity eluent ($\eta = 0.5$ cP). Therefore, it appears very challenging to run fast and efficient capillary columns of diameter smaller than 300 μm for the analysis of small molecules. To solve these problems, injection and detection should be performed directly on-column in nano-fluidic devices. To run fast chromatography, these capillary channels packed with 1 μm particles need to be prepared in a block, which could support pressures up to 5–10 kbar.

5. Conclusion

This work elaborate on the rapid progress of column performance that have taken place during the last ten years of intense development in column technology that we have witnessed. After the early success of the first generation of highly permeable monolithic columns, enthusiasm faded but a new generation of sub-2 μm fully porous particles combined with improved vHPLC instruments allowed the production of columns that generated a twice higher resolution at constant analysis time or a four-fold reduction of the time needed for analyses providing the same peak resolution. The failure of the first generation of monolithic columns is directly related to the structure heterogeneity of the 4.6 mm I.D. rods and to the poor distribution of the sample molecules at the column inlet. Eventually, peaks are tailing and no more than 60 000 true plates per meter are available. Chromatographers are patiently waiting for a second generation of monolithic columns, currently announced to come in a 3.0 mm I.D. format, only.

The most remarkable progress in column technology was unexpected. It came in late 2007, with the introduction of the sub-3 μm core–shell particles. The original incentive for the research and development made on the production of such particles was triggered by efforts to reduce the average solute diffusion path across the particles of a packed bed while maintaining a sufficiently large specific surface area, hence the column saturation capacity. It eventually turned out that, at least for small molecules, the improvement observed in the trans-particle mass transfer was marginal because this source of mass transfer resistance is small for all but the largest molecules [86]. In contrast, it was that most of the remarkable increase in the efficiencies of these columns in the velocity range around the optimum for minimum HETP was brought up by a strong diminution of the eddy diffusion term. So far, both experimental and theoretical data that we acquired agree to conclude that the smaller eddy diffusion term observed for columns packed with these shell particles in 4.6 mm I.D. columns is due to a decrease of the conventional trans-column eddy diffusion term (the so-called wall effects) and that this is a consequence of the external roughness of these particle. Eventually, for a conventional 400 bar inlet pressure, columns packed with sub-3 μm shell particles can provide at least the same or often better chromatographic performance than those columns packed of sub-2 μm fully porous particles, according to the extrapolated kinetic Poppe plots.

It seems that the minimum value of the reduced HETP that we could reasonably expect to ever achieved is of the order of one. The best columns packed with shell particles with which we have worked yielded minimum values of their HETP between 1.1 and 1.3. This suggests that beyond what a fine tuning of the packing procedure could eventually provide, little further gain in column efficiency can be expected. A few other approaches remain to be explored. Operating columns at elevated temperatures appears to be the most practical solution towards faster, efficient separations. An eluent viscosity of 0.35 cP (such as pure acetonitrile at room temperature or aqueous mixtures of acetonitrile and water at moderate temperatures) can provide hold-up times of the order of one second with 2.1 mm × 50 mm columns packed with 1.7 μm core–shell materials at an operating pressure of 1000 bar. Such a column could generate apparent efficiencies between 2500 and 3000 plates for weakly retained compounds ($k = 1$), which in gradient elution of small molecules, would translate into intrinsic a peak capacity of ca. 40 within about 15 s with a relatively smooth gradient steepness ($G = S\beta t_0 \simeq 0.2$). Obviously, this performance would be affected by the large volume injected into the column (in LC × LC, this volume could be at least around 20 μL), and the eluent mismatch between the injected sample and the eluent (often the case in LC × LC which uses orthogonal dimensions). Yet, such speed/resolution performance is definitely achievable today with the best R & D products available in analytical chromatography.

Future progress might be expected in the analysis of large biomolecules during the next decade. Although faster chromatography of small molecules could remains a possibility with a generation of 1 μm particles, it is not sure whether the large investments needed to implement it will be made. As the emergence of the sub-2 μm particles in 2004 required new vHPLC instruments, a new generation of instruments, having greatly reduced extra-column band broadening contributions and capable of operating up to 5 kbar will be necessary to operate columns packed with 1 μm particles; the negative impact of frictional heating on column efficiency could be solved by using 1.0 mm I.D. columns (microflow) or by replacing the conventional shell particles with a silica core in 2.1 mm I.D. narrow-bore columns with a particles made of a core having a larger thermal conductivity around 50 W/m/K, such as alumina or an equivalent material. Then procedures must be developed to pack 1 μm shell particles into sub-1 mm I.D. columns and achieve the same efficiency as those of current 4.6 mm I.D. columns. Yet, the difficult problem will be to decide whether it is possible to develop micro- or nano-flow HPLC systems able to operate at such high inlet pressures and if it is worth to do so. On the other hand, however, the use of 1 μm shell particles for the analysis of biopolymers seems highly probable because the difficulties are far simpler to solve. The optimum reduced velocity of these columns will remain the same as they are now for low molecular weight compounds, around 10. But for biopolymers, which have a high molecular weight, this reduced velocity corresponds to a lower actual mobile phase flow rate, several times, up to ten times lower, since the optimum actual velocity is proportional to the diffusion coefficient. Thus, the same columns should be used at much lower flow rates and current vHPLC instruments can do.

List of symbols

Roman letters

A	Eddy diffusion plate height (m)

A_η empirical parameter in Eq. (10)
B longitudinal diffusion coefficient (m^2/s)
B_η empirical parameter in Eq. (10) (K)
C_i discreet sample concentration in the recorded concentration profile (kg/m^3)
C solid–liquid mass transfer coefficient (s)
d_p mean particle diameter (m)
D_m bulk molecular diffusion coefficient (m^2/s)
F_{Film} empirical parameter in Eq. (14)
F_v flow rate (m^3/s)
G intrinsic gradient steepness
H total column HETP (m)
H_{Film} external film mass transfer resistance term (m)
$H_{stat.}$ trans-particle particle mass transfer resistance HETP term (m)
k retention factor
k_1 zone retention factor
k_0 specific permeability (m^2)
k_F apparent retention factor of the last eluted peak in gradient elution
L column length (m)
N column efficiency
P_c peak capacity
ΔP pressure drop along the column (Pa)
r_c column inner radius (m)
S linear strength model slope
t_G gradient time (s)
t_0 column hold-up time (s)
T temperature (K)
T_{Ref} reference temperature (K)
ΔT amplitude of the radial temperature gradient (K)
t_i discreet time variable in the recorded concentration profile (s)
u_{opt} optimal interstitial linear velocity (m/s)
u_S superficial linear velocity (m/s)
V_0 column hold-up volume (m^3)

Greek letters

α_P isobaric thermal expansion coefficient (K^{-1})
β gradient steepness (s^{-1})
ϵ_e external column porosity
ϵ_t total column porosity for non-excluded analytes
η eluent viscosity (Pa s)
$\Delta\varphi$ variation of the volume fraction of the strong eluent during the gradient time
κ parameter in Eq. (19)
λ flow-related parameter in the Giddings' eddy diffusion Eq. (13)
λ_p effective thermal conductivity of the packed bed immersed in the eluent (W/m/K)
μ_1 experimental first moment in presence of column (s)
$\mu_{1,ex}$ first moment of the extra-column band profiles (column replaced with a zero volume union connector) (s)
μ'_2 experimental second central moment in presence of column (s^2)
$\mu'_{2,ex}$ second central moment of the extra-column band profiles (column replaced with a zero volume union connector) (s^2)
ω diffusion-related parameter in the Giddings' eddy diffusion Eq. (13)
Ω ratio of the sample diffusivity in the porous shell to the bulk diffusion coefficient
Ψ parameter in Eq. (19)
ν_S superficial reduced linear velocity
$\sigma^2_{v,column}$ volume variance contribution of the column (m^6)

Acknowledgements

This work was supported in part by the cooperative agreement between the University of Tennessee and the Oak Ridge National Laboratory.

References

[1] F. Gritti, G. Guiochon, Anal. Chem. 78 (2006) 5329.
[2] K.K. Unger, G. Jilge, J.N. Kinkel, M.T.W. Hearn, J. Chromatogr. 359 (1986) 61–72.
[3] K.K.H. Moriyama, M. Anegayama, Y. Kato, J. Chromatogr. A 691 (1995) 81–89.
[4] G. Guiochon, J. Chromatogr. A 1168 (2007) 101.
[5] K. Nakanishi, N. Soga, J. Am. Ceram. Soc. 74 (1991) 2518.
[6] H. Minakuchi, K. Nakanishi, N. Soga, N. Ishizuka, N. Tanaka, Anal. Chem. 68 (1996) 3498.
[7] F. Gritti, W. Piatkowski, G. Guiochon, J. Chromatogr. A 978 (2002) 81.
[8] M. Kele, G. Guiochon, J. Chromatogr. A 960 (2002) 19.
[9] F. Gritti, G. Guiochon, J. Chromatogr. A, 1218 (2011) 5216.
[10] H. Minakuchi, K. Nakanishi, N. Soga, N. Ishizuka, N. Tanaka, J. Chromatogr. A 762 (1997) 135.
[11] H. Minakuchi, K. Nakanishi, N. Soga, N. Ishizuka, N. Tanaka, J. Chromatogr. A 797 (1998) 121.
[12] F. Gritti, W. Piatkowski, G. Guiochon, J. Chromatogr. A 983 (2003) 51.
[13] Proceedings of the 32nd International Symposium on High Performance Liquid Phase Separations and Related Techniques, Baltimore, MD, May 10–16, 2008.
[14] F. Gritti, G. Guiochon, J. Chromatogr. A 1216 (2009) 1353.
[15] F. Gritti, G. Guiochon, J. Chromatogr. A 1217 (2010) 1485.
[16] K. Mriziq, J. Abia, Y. Lee, G. Guiochon, J. Chromatogr. A 1193 (2008) 97.
[17] K. Cabrera, J. Sep. Sci. 27 (2004) 843.
[18] J. Abia, K. Mriziq, G. Guiochon, J. Chromatogr. A 1216 (2009) 3185.
[19] F. Gritti, G. Guiochon, J. Chromatogr. A 1216 (2009) 4752.
[20] C. Horváth, S.R. Lipsky, J. Chromatogr. Sci. 7 (1969) 109.
[21] J.J. Kirkland, Anal. Chem. 41 (1969) 218.
[22] J.J. Kirkland, Anal. Chem. 64 (1992) 1239.
[23] J.J. DeStefano, T.J. Langlois, J.J. Kirkland, J. Chromatogr. Sci. 46 (2007) 254–260.
[24] F. Gritti, I. Leonardis, D. Shock, P. Stevenson, A. Shalliker, G. Guiochon, J. Chromatogr. A 1217 (2010) 1589.
[25] F. Gritti, G. Guiochon, J. Chromatogr. A 1217 (2010) 1604.
[26] F. Gritti, I. Leonardis, J. Abia, G. Guiochon, J. Chromatogr. A 1217 (2010) 3819.
[27] F. Gritti, G. Guiochon, J. Chromatogr. A 1218 (2011) 1915.
[28] J.O. Omamogho, J.P. Hanrahan, J. Tobin, J.D. Glennon, J. Chromatogr. A 1218 (2011) 1942.
[29] L. Blue, J. Jorgenson, Synthesis and characterization of 1.1 μm superficially porous particles for liquid chromatography, Anal. Chem. 83,submitted for publication.
[30] F. Gritti, G. Guiochon, Chem. Eng. Sci. 65 (2010) 6310.
[31] F. Gritti, G. Guiochon, J. Chromatogr. A 1217 (2010) 5069.
[32] F. Gritti, C. Sanchez, T. Farkas, G. Guiochon, J. Chromatogr. A 1217 (2010) 3000.
[33] F. Gritti, G. Guiochon, J. Chromatogr. A, 1218 (2011) 4452.
[34] H. Poppe, J. Chromatogr. A 778 (1997) 3.
[35] V. Wong, R.A. Shalliker, G. Guiochon, Anal. Chem. 76 (2004) 2601.
[36] F. Gritti, G. Guiochon, J. Chromatogr. A 1070 (2005) 13.
[37] F. Gritti, G. Guiochon, J. Chromatogr. A 1070 (2005) 1.
[38] F. Gritti, G. Guiochon, J. Chromatogr. A 1075 (2005) 117.
[39] M. Martin, G. Guiochon, J. Chromatogr. A 1090 (2005) 16.
[40] F. Gritti, G. Guiochon, J. Chromatogr. A 1187 (2008) 165.
[41] F. Gritti, G. Guiochon, Anal. Chem. 80 (2008) 5009.
[42] F. Gritti, G. Guiochon, Anal. Chem. 80 (2008) 6488.
[43] F. Gritti, G. Guiochon, J. Chromatogr. A 1206 (2008) 113.
[44] G. Guiochon, A. Felinger, A. Katti, D. Shirazi, Fundamentals of Preparative and Nonlinear Chromatography, 2nd ed., Academic Press, Boston, MA, 2006.
[45] F. Gritti, G. Guiochon, AIChE J. 56 (2010) 1495.
[46] F. Gritti, G. Guiochon, J. Chromatogr. A 1218 (2011) 907.
[47] F. Gritti, Y. Kazakevich, G. Guiochon, J. Chromatogr. A 1161 (2007) 157.
[48] F. Gritti, Y. Kazakevich, G. Guiochon, J. Chromatogr. A 1169 (2007) 111.
[49] J. Li, P. Carr, Anal. Chem. 69 (1997) 2530.
[50] J. Li, P. Carr, Anal. Chem. 69 (1997) 2550.
[51] B. Poling, J. Prausnitz, J. O'Connel, The Properties of Gases and Liquids, 5th ed., McGraw-Hill, New York, NY, 2001.
[52] J. Giddings, Dynamics of Chromatography, Marcel Dekker, New York, NY, 1965.
[53] C. Wilke, P. Chang, AIChE J. 1 (1955) 264–270.
[54] T. Weber, T.P. Jackson, P. Carr, Anal. Chem. 67 (1995) 3042.
[55] J.W. Li, Y. Hu, P. Carr, Anal. Chem. 69 (1997) 3884.
[56] P. Zhao, P. Carr, Anal. Chem. 70 (1998) 3619.
[57] B. Yan, J. Zhao, J. Brown, J. Blackwell, P. Carr, Anal. Chem. 72 (2000) 1253.
[58] Y. Xiang, B. Yan, B. Yue, C. McNeff, P. Carr, M. Lee, Anal. Chem. 72 (2000) 1253.
[59] G. Guiochon, A. Tarafder, J. Chromatogr. A 1218 (2011) 1017.
[60] A. Tarafder, G. Guiochon, J. Chromatogr. A 1218 (2011) 7189.
[61] D.P. Poe, J.J. Schroden, J. Chromatogr. A 1216 (2009) 7915.
[62] D. Poe, J. Schroden, J. Chromatogr. A 1216 (2009) 7915.
[63] K. Kaczmarski, D. Poe, G. Guiochon, J. Chromatogr. A 1217 (2010) 6578.
[64] K. Kaczmarski, D.P. Poe, G. Guiochon, J. Chromatogr. A 1218 (2011) 6531.

[65] F. Gritti, G. Guiochon, J. Chromatogr. A, 1218 (2011) 4632.
[66] F. Gritti, M. Martin, G. Guiochon, Anal. Chem. 81 (2009) 3365.
[67] J.F.K. Huber, private communication.
[68] F. Gritti, G. Guiochon, J. Chromatogr. A 1217 (2010) 7677.
[69] A. Daneyko, A. Holtzel, S. Khirevich, U. Tallarek, Anal. Chem., 83 (2011) 3903.
[70] F. Gritti, G. Guiochon, Chem. Eng. Sci. 65 (2010) 6327.
[71] J. Kostka, F. Gritti, K. Kaczmarski, G. Guiochon, J. Chromatogr. A 1217 (2010) 4704.
[72] J. Kostka, F. Gritti, K. Kaczmarski, G. Guiochon, J. Chromatogr. A 1218 (2011) 5449.
[73] H. Poppe, J. Paanaker, M. Bronckhorst, J. Chromatogr. 204 (1981) 77.
[74] L. Snyder, High Performance Liquid Chromatography – Advances and Perspectives, Elsevier, Amsterdam, 1986.
[75] U.D. Neue, J. Chromatogr. A 1079 (2005) 153.
[76] J. Nawrocki, C. Dunlap, J. Li, J. Zhao, C.V. McNeff, A. McCormick, P.W. Carr, J. Chromatogr. A. 1038 (2004) 31.
[77] X. Yang, L. Ma, P.W. Carr, J. Chromatogr. A 1079 (2005) 213.
[78] K.D. Patel, A.D. Jerkovich, J.C. Link, J.W. Jorgenson, Anal. Chem. 76 (2004) 5777.
[79] J.S. Mellors, J.W. Jorgenson, Anal. Chem. 76 (2004) 5441.
[80] J.E. MacNair, K.D. Patel, J.W. Jorgenson, Anal. Chem. 71 (1999) 700.
[81] J.E. MacNair, K.C. Lewis, J.W. Jorgenson, Anal. Chem. 69 (1997) 983.
[82] F. Gritti, G. Guiochon, J. Chromatogr. A 1166 (2007) 47.
[83] H. Poppe, J.C. Kraak, J.F.K. Huber, J.H.M. Van Den Berg, Chromatographia 14 (1981) 515.
[84] Y.P. Zarichnyak, V.V. Novikov, Inzh. -Fizi. Zh. 34 (1978) 648.
[85] F. Gritti, G. Guiochon, J. Chromatogr. A, submitted for publication.
[86] K. Kaczmarski, G. Guiochon, Anal. Chem. 79 (2007) 4648.